

Effective Field Theory for Two-Body Systems with Shallow S -Wave Resonances

J. Balal Habashi and S. Fleming

Department of Physics, University of Arizona, Tucson, AZ 85721, USA

S. Sen

Department of Physics & Astronomy, Iowa State University, Ames, IA 50011, USA

U. van Kolck

*Université Paris-Saclay, CNRS/IN2P3, IJCLab, 91405 Orsay, France and
Department of Physics, University of Arizona, Tucson, AZ 85721, USA*

Resonances are of particular importance to the scattering of composite particles in quantum mechanics. We build an effective field theory for two-body scattering which includes a low-energy S -wave resonance. Our starting point is the most general Lagrangian with short-range interactions. We demonstrate that these interactions can be organized into various orders so as to generate a systematic expansion for an S matrix with two low-energy poles. The pole positions are restricted by renormalization at leading order, where the common feature is a non-positive effective range. We carry out the expansion explicitly to next-to-leading order and illustrate how it systematically accounts for the results of a toy model — a spherical well with a delta shell at its border.

I. INTRODUCTION

In quantum mechanics, observables are encoded in the S matrix or, equivalently, in the T matrix. In the complex momentum plane, poles of the S matrix lying on the positive imaginary axis with positive residue correspond to bound states [1], while poles on the negative imaginary axis are negative-energy virtual states, which are not normalizable. Pairs of poles can also appear at complex momentum with equal, negative imaginary parts and equal but opposite real parts. These poles can be thought of as resonance states with a finite lifetime¹, which affect scattering significantly when they lie close to the real axis. Resonances are common in the nonrelativistic scattering of atoms and nuclei, sometimes appearing in the S wave (see, for example, Ref. [2]). Shallow resonances can lead to significant variation of phase shifts at low energies. Examples include a very low-energy resonance in proton-proton scattering [3] and the ^8Be ground state in the scattering of two alpha particles [4]. Here we develop a systematic treatment of shallow S -wave resonances, or more generally two shallow poles, based on effective field theory (EFT).

EFTs exploit a separation of scales to generate a controlled expansion of observables in the small ratio(s) of these scales. The EFT framework was originally formulated in particle physics to allow a perturbative treatment of low-energy processes involving strong-interacting particles [5], and immediately used to justify the successes of the perturbative Standard Model despite the wide range of possibilities for its underlying dynamics [6]. In the 1990s, as it was being applied to nuclear physics (for a review, see for example Refs. [7, 8]), the need arose for EFT to be extended to shallow, nonrelativistic bound and virtual states, which cannot be treated in perturbation theory. Originally motivated by the two-nucleon problem, which exhibits a bound state in one S wave and a virtual state in another, an EFT description of shallow S -wave two-body states was achieved in the late 1990s [9–12]. This was possible using either momentum-dependent contact interactions or a “dimeron” auxiliary field [13], which gives rise to energy-dependent interactions. Within a few years, shallow two-body resonances also yielded to an EFT approach, but only with a “dimeron” field [14–18]. While the corresponding energy-dependent interactions could be used in three-body calculations [19–21], they are not easily incorporated in most *ab initio* methods that enable the solution of the Schrödinger (or equivalent) equation for more than three particles. Our goal here is to extend the EFT of shallow S -wave two-body resonances to momentum-dependent interactions, which should find wider use.

To understand two-body resonant scattering at low energy in an EFT framework we need to identify the characteristic momentum scales inherent to the process². We consider the scattering of two particles at a momentum $k \sim M_{l_o}$ which is much smaller than the inverse range of the interaction $1/R \sim M_{h_i}$. In the nonrelativistic regime, this problem is equivalent to the scattering of a particle by a potential of finite range, but one in which the particle cannot resolve the details of the potential. It is sensible to make a “multipole” expansion of the potential, which

¹ We refer to a pole at complex (neither real nor purely imaginary) momentum as a “resonance”, regardless of whether it generates a bump in a cross section.

² We use units such that $\hbar = c = 1$, so that mass, momentum, energy, inverse distance, and inverse time all have the same dimensions.

can be considered as a sum of Dirac delta functions with an increasing number of derivatives. Such a potential can be formulated in terms of the most general Lagrangian density involving only the fields associated with the particles under study. The two-body potential is generated by interactions that involve four fields at the same spacetime point and their derivatives. The coefficient of an operator with n derivatives — called Wilson coefficient in the particle physics literature and low-energy constant (LEC) in hadronic and nuclear physics — is a real number $4\pi C_n/m$ that encodes the details of the short-range dynamics. Here we consider for simplicity a single particle species of mass m and the most common case where the underlying dynamics is not only Lorentz invariant, but also symmetric under spatial parity and time reversal. We also neglect spin degrees of freedom, which bring no essential complications. In this case only interactions with an even number of derivatives appear. The more general case can be obtained straightforwardly following the same steps as we do below.

We show in the following how scattering around a resonance can be described systematically in a series in powers of M_{lo}/M_{hi} , regardless of the details of the underlying interaction, as long as its range is short compared to the magnitude of the inverse momentum of the resonance. The two-body dynamics at low energies is obtained via the selective resummation of Feynman diagrams, or equivalently by solving the Schrödinger equation. In either case, as is usual in field theory, one has to impose a regularization procedure to cope with the singularity of the interactions. The conceptually simplest regularization, which we employ below, imposes a momentum cutoff Λ . The choice of regulator is arbitrary and thus makes for a particular model of the short-range dynamics. To ensure observables are insensitive to this arbitrary choice and model independent, the theory has to be renormalized. The Λ dependence of each “bare” LEC that appears in the Lagrangian, $4\pi C_n(\Lambda)/m$, is determined by imposing that a low-energy observable be Λ independent. Other low-energy observables then depend on Λ only through positive powers of $1/\Lambda$ and approach finite limits as $\Lambda \gg M_{hi}$. The expansion is organized in such a way that renormalization holds at each order, up to terms that have the same magnitude as higher-order terms when $\Lambda \gtrsim M_{hi}$. Thus, we can reproduce the effects of any potential exhibiting a shallow resonance to arbitrary accuracy.

The choice of low-energy observables used in the renormalization procedure is equally arbitrary, up to higher-order terms. A particularly simple choice is offered by the effective-range expansion (ERE) [22]. From general considerations it is possible to show [12] that an EFT for short-range interactions leads to a T matrix for S -wave scattering at on-shell momentum $k \ll R^{-1}$ which can be expressed in the ERE form

$$T_0(k) = -\frac{4\pi}{m} (k \cot \delta_0(k) - ik)^{-1} = -\frac{4\pi}{m} \left[-\frac{1}{a_0} + \frac{r_0}{2} k^2 - P_0 \left(\frac{r_0}{2} \right)^3 k^4 + \dots - ik \right]^{-1}, \quad (1)$$

where $\delta_0(k)$ is the phase shift, and a_0, r_0, P_0, \dots are known as, respectively, scattering length, effective range, shape parameter³, *etc.* The values of the ERE parameters can be extracted from the phase shifts, which in turn can be obtained from data with only mild theoretical input. As is done in much of the EFT literature [7, 8], we fix the LECs by forcing them to agree with the empirical values of these ERE parameters: C_0 is related to the scattering length, C_2 to the effective range, *etc.*

A crucial aspect of EFT is “power counting” — the argument that justifies the expansion of the amplitude in powers of M_{lo}/M_{hi} or “orders”: leading order (LO), next-to-leading order (NLO), next-to-next-to-leading order (N²LO), and so on. The simplest assumption is that of “naturalness”, where the size of observables is set solely by the large momentum scale M_{hi} : $|a_0| \sim 1/M_{hi}$, $|r_0| \sim 1/M_{hi}$, $|P_0| \sim 1$, *etc.* (For a review, see Ref. [23].) This is assured if the renormalized LECs scale as $C_n = \mathcal{O}(1/M_{hi}^{n+1})$. In this case $T_0(k)$ is purely perturbative, with LO consisting of C_0 in first order in perturbation theory, NLO of C_0 in second order, N²LO of C_0 in third order and C_2 in first order, and so on. (Starting at N²LO contributions to higher waves are also present.) Poles characterized by momentum $|k| \ll M_{hi}$ thus require a certain amount of fine tuning in the underlying theory such that at least one interaction is large enough to demand a nonperturbative treatment.

It is relatively easy to find examples of a fine tuning that produces a large scattering length, $|a_0| \sim 1/M_{lo} \gg 1/M_{hi}$. This situation corresponds to a single, shallow S -wave bound or virtual state near threshold. This is an intrinsically quantum-mechanical phenomenon: the particles in the bound state are on average at distances much larger than the range of the interaction, which in classical physics determines the size of orbits. For example, for a square well of fixed range R , one can produce such states at values of the depth β^2/mR^2 for which β is close to an odd multiple of $\pi/2$. In this case, the LECs scale as $C_0 = \mathcal{O}(1/M_{lo})$ and $C_{n \geq 2} = \mathcal{O}(1/M_{lo}^2 M_{hi}^{n-1})$ [9–12]. For $k \sim 1/|a_0|$, the interaction with no derivatives and coefficient C_0 is as important as the unitarity term ik , and it needs to be treated nonperturbatively. All remaining terms in the ERE can still be treated as perturbations in a distorted-wave Born expansion. The resulting S -wave T matrix is an expansion of Eq. (1). It yields either a bound state or a virtual state,

³ In much of the literature the coefficient of k^4 is defined to be $P_0 r_0^3$. With our choice P_0 takes on more natural values.

depending on the sign of the scattering length, at $k \simeq i/a_0 \sim \pm iM_{lo}$. This is exactly what happens in nucleon-nucleon scattering at low energies. Just as in the natural case, higher waves appear at higher orders.

Neither of these two power-counting schemes can produce a shallow resonance. For this to occur we need, in general, to have two fine tunings, with $|a_0| \sim 1/M_{lo}$ and $|r_0| \sim 1/M_{lo}$. We expect the physics of such a scaling to be produced by an effective Lagrangian where the two leading operators in the derivative expansion are of a size much larger than what is expected from naturalness and hence have to be treated nonperturbatively. In contrast to other cases, $C_0 = \mathcal{O}(1/M_{lo})$ and $C_2 = \mathcal{O}(1/M_{lo}^3)$, with other LECs smaller, being suppressed by powers of M_{hi} . We will argue that $C_{n \geq 4} = \mathcal{O}(1/M_{lo}^{n/2+2} M_{hi}^{n/2-1})$. These are the central ideas of our paper.

Proper renormalization is the cornerstone of our approach. This is not the first time that the two leading contact interactions are solved exactly. In fact our LO solution reproduces the amplitude of Beane, Cohen, and Phillips [24, 25]. These authors have shown that renormalization requires $r_0 \lesssim 1/\Lambda$ for $\Lambda \gg M_{lo}$, which is an example of Wigner’s bound on phase shifts [26]. However, in those early days of nuclear EFT, Beane *et al.* were concerned with bound states. The fact that two-nucleon data require $r_0 > 0$ led those authors to conclude that EFT was of little use in a nonperturbative context. Later, it was shown [9–12] that in the case of a single shallow bound or virtual state the two-derivative interaction should not be iterated to all orders⁴ and, when treated perturbatively, it can accommodate either sign of r_0 . Like Beane *et al.*, we take renormalizability and its constraint $r_0 \leq 0$ seriously. However, here we note that we are dealing with a valid EFT — just not one with a single fine tuning as relevant in the two-nucleon problem, but the case where the underlying theory has the two fine tunings needed for an S -wave resonance or, more generally, two low-energy poles.

With this interpretation, we use the power counting outlined above to predict the positions of poles with controlled errors, which can be improved by adding higher-order operators perturbatively to the LO effective Lagrangian. The renormalization requirement $r_0 \leq 0$ forces resonance poles to be in the lower half of the complex-momentum plane, which guarantees their role as decaying states. More generally, there are two T -matrix poles, the positions of which are determined in the complex momentum plane by the relative sizes of a_0 and $r_0 \leq 0$. The two poles can lie

- both below the real axis with non-vanishing, equal and opposite real parts — a resonance;
- on top of each other on the negative imaginary axis — a double virtual pole;
- both on the negative imaginary axis, but separated — two virtual states;
- one on the negative imaginary axis and the other at the origin — a virtual state and a “zero-energy resonance”;
or
- one on the negative and the other on the positive imaginary axis — one virtual and one bound state.

At NLO, the four-derivative contact interaction enters, which leads to the shape parameter $|P_0| \sim M_{lo}/M_{hi}$. We demonstrate the systematic character of our approach by considering an example where the underlying interaction takes a particularly simple form: a spherical well of range R with a delta-shell potential at its edge. By varying the strengths of the two components of the underlying potential at fixed R we can produce two poles in each of the arrangements mentioned above. Fixing the EFT parameters from the ERE parameters that appear at each order, we show how the toy-model phase shifts and pole positions are approximated with increasing accuracy when we go from LO to NLO. In the future we hope to include the Coulomb interaction as well, so as to be able to consider not only a toy model, but also an S -wave resonance of phenomenological interest such as the ${}^8\text{Be}$ ground state.

The organization of the paper is as follows. In Sec. II we show the form of the relevant effective Lagrangian in the derivative expansion, as well as the potential in LO and NLO. In Sec. III we derive the scattering amplitude for the EFT at LO using the Schrödinger equation, followed by the nonperturbative renormalization of the bare parameters $C_0(\Lambda)$ and $C_2(\Lambda)$ of the two leading operators in the effective Lagrangian. We then find the scattering amplitude for the EFT at NLO and perturbatively renormalize the amplitude using $C_4(\Lambda)$, the bare parameter of the four-derivative contact interaction. (An alternative derivation of the results of this section using field theory is offered in App. A, while some details of the renormalization procedure are given in App. B.) In the following section, Sec. IV, we demonstrate that our EFT successfully reproduces shallow resonant states in the ERE. We also analyze the sensitivity of the positions of the poles for bound and virtual states to perturbations, and the error in the position of the poles is estimated. We compare in Sec. V the results from EFT with those of a toy model which among other states includes two shallow poles. We conclude in Sec. VI.

⁴ For a recent proposal on how to iterate corrections in limited cutoff ranges while retaining the EFT expansion, see Ref. [27].

II. EFT FOR TWO-BODY SCATTERING

In this section we construct an EFT for scattering that exhibits a shallow S -wave resonance. The energy of scattering particles is restricted to be on the order of the resonance energy, assumed to correspond to momentum much smaller than the inverse of the underlying interaction range. The scattering process is assumed to be elastic, meaning there is a single open channel with particles taken to be in their ground states both before and after scattering. (For scattering with more open channels, see Ref. [28].) For simplicity we limit ourselves to one particle species not affected by the exclusion principle, but generalization is straightforward. As a consequence, we are concerned with a single “heavy” field [29] ψ , which encodes the annihilation of a particle, and contact operators in the Lagrangian that are Hermitian, as there is no source or sink. Furthermore, our EFT is invariant under Lorentz (in the form of reparameterization invariance [30]), parity and time-reversal transformations, and conserves particle number. The most general Lagrangian for scattering without spin which respects these symmetries and constraints can be written in the form [31]

$$\begin{aligned} \mathcal{L} = & \psi^\dagger \left(i \frac{\partial}{\partial t} + \frac{\vec{\nabla}^2}{2m} + \dots \right) \psi - \frac{4\pi}{m} \left\{ C_0 (\psi\psi)^\dagger (\psi\psi) - \frac{C_2}{8} [(\psi\psi)^\dagger (\psi \overleftrightarrow{\nabla}^2 \psi) + \text{H.c.}] \right. \\ & \left. + \frac{C_4}{64} [(\psi\psi)^\dagger (\psi \overleftrightarrow{\nabla}^4 \psi) + \text{H.c.} + 2 (\psi \overleftrightarrow{\nabla}^2 \psi)^\dagger (\psi \overleftrightarrow{\nabla}^2 \psi)] + \dots \right\}, \end{aligned} \quad (2)$$

where $\overleftrightarrow{\nabla} \equiv \overrightarrow{\nabla} - \overleftarrow{\nabla}$. Here we display explicitly only terms contributing to the (on-shell) S -wave scattering of two particles: the term quadratic in the field ψ is the nonrelativistic kinetic term, while the others correspond to interactions with LECs $4\pi C_n/m$. The “...” represent operators with more derivatives and fields, and/or operators that only contribute to two-body scattering off shell and in higher partial waves. For example, there is an independent operator with four derivatives, which vanishes when the two-body system is on shell [32], which allows us to take the coefficient of $(\psi \overleftrightarrow{\nabla}^2 \psi)^\dagger (\psi \overleftrightarrow{\nabla}^2 \psi)$ to be $-\pi C_4/8m$ [31]. Similar choices can be made for higher-derivative operators. Interactions that vanish on shell in the two-body system cannot be separated from operators involving more fields, for example three-body forces of the type $(\psi^\dagger \psi)^3$. Since we have integrated out antiparticles, operators with six or more fields do not contribute to the two-body system.

For simplicity we work in the center-of-mass frame, where the scattering particles have relative momenta \vec{p} and \vec{p}' before and after scattering, respectively. From the Feynman diagrams corresponding to the Lagrangian (2) we can obtain the nonrelativistic potential in momentum space [12, 24, 25],

$$\langle \vec{p}' | \hat{V} | \vec{p} \rangle = \frac{4\pi}{m} \left[C_0 + \frac{C_2}{2} (\vec{p}'^2 + \vec{p}^2) + \frac{C_4}{4} (\vec{p}'^2 + \vec{p}^2)^2 + \dots \right], \quad (3)$$

and, from that, the potential in coordinate space,

$$\begin{aligned} \langle \vec{r}' | \hat{V} | \vec{r} \rangle = & \frac{4\pi C_0}{m} \delta(\vec{r}') \delta(\vec{r}) - \frac{2\pi C_2}{m} [(\nabla'^2 \delta(\vec{r}')) \delta(\vec{r}) + \delta(\vec{r}') (\nabla^2 \delta(\vec{r}))] \\ & + \frac{\pi C_4}{m} [(\nabla'^4 \delta(\vec{r}')) \delta(\vec{r}) + 2 (\nabla'^2 \delta(\vec{r}')) (\nabla^2 \delta(\vec{r})) + \delta(\vec{r}') (\nabla^4 \delta(\vec{r}))] + \dots \end{aligned} \quad (4)$$

Our first task is to order these interactions according to their effects on observables. In general the same operator contributes to various orders, so we decompose the LECs as

$$C_n = C_n^{(0)} + C_n^{(1)} + \dots, \quad (5)$$

where $C_n^{(N)}$ is the part of C_n that contributes at order N .

Since we are interested in situations where there are two low-energy S -wave poles, the denominator of the LO scattering amplitude must be quadratic in momentum. In our EFT with momentum-dependent interactions we need to treat both C_0 and C_2 nonperturbatively (*i.e.* at LO) to reproduce this non-analytic behavior. In momentum space, the LO potential is therefore

$$\langle \vec{p}' | \hat{V}^{(0)} | \vec{p} \rangle = \frac{4\pi}{m} \left[C_0^{(0)} + \frac{C_2^{(0)}}{2} (\vec{p}'^2 + \vec{p}^2) \right]. \quad (6)$$

In other words, $C_{n \geq 4}^{(0)} = 0$. We seek an exact, nonperturbative solution of this potential under a momentum cut-off regulator Λ , with $C_{0,2}^{(0)}(\Lambda)$ determined from the requirement that two observable quantities be reproduced.

At higher orders, we expect small, perturbative corrections from higher-derivative operators. The fact that zero- and two-derivative operators are taken as LO might suggest that there is no expansion that suppresses the higher-derivative operators. However, as discussed in the introduction, we are facing a fine-tuned situation where a low-energy scale M_{l_o} enhances all operators, but not in the same way. Subleading interactions are suppressed by powers of the high-energy scale M_{hi} , which are not entirely obvious at first. A powerful guide in this situation is the renormalization group (RG). At any given order, observables not used in the determination of LECs have residual cutoff dependence: they depend on M_{l_o} and M_{hi} in a form dictated by the explicit solution of the EFT interactions up to that order, and additionally on inverse powers of Λ . This residual cutoff dependence will be removed at higher orders by other LECs, which will have bare components that scale as inverse powers of Λ . Naturalness assumes that the magnitude of a renormalized LEC is determined by changes in the cutoff of relative $\mathcal{O}(1)$. This implies that for cutoffs that do not intrude in the region where we want the EFT to converge, $\Lambda \gtrsim M_{hi}$, we can determine the magnitude of the renormalized LEC, and hence its order, by the replacement $\Lambda \rightarrow M_{hi}$ in the bare LEC.

We will show below that the assumption of naturalness for subleading operators leads to a controlled expansion. In particular, the NLO momentum-space potential is

$$\langle \vec{p}' | \hat{V}^{(1)} | \vec{p} \rangle = \frac{4\pi}{m} \left[C_0^{(1)} + \frac{C_2^{(1)}}{2} (\vec{p}'^2 + \vec{p}^2) + \frac{C_4^{(1)}}{4} (\vec{p}'^2 + \vec{p}^2)^2 \right], \quad (7)$$

which is to be treated in first-order perturbation theory. The appearance of quartic momentum operators at this order means that an additional observable is needed to fix $C_4^{(1)}(\Lambda)$. The latter induces changes in the observables fitted at LO. To compensate, we include perturbative changes in $C_{0,2}$ so that $C_{0,2}^{(1)}(\Lambda)$ produce opposite changes in these observables, which then remain fixed at the values chosen at LO. For the remaining interactions, $C_{n \geq 6}^{(1)} = 0$.

An analogous procedure is followed at higher orders. The removal of regularization dependence — up to effects no larger than those of the truncation in the potential — can be performed by a finite number of parameters *at each order*. That means that the theory is renormalizable in the modern sense, which generalizes the old-fashioned concept of a finite set of interactions at all orders.

III. SOLVING THE SCHRÖDINGER EQUATION

Equipped with the potential we now obtain the S -wave scattering amplitude in an expansion

$$T_0(k) = T_0^{(0)}(k) + T_0^{(1)}(k) + \dots, \quad (8)$$

where successive terms are suppressed by an additional power of M_{l_o}/M_{hi} . In order to renormalize the resulting amplitude, we demand that the $C_n^{(N)}(\Lambda)$ appearing in the expansion

$$\frac{1}{T_0(k)} = \frac{1}{T_0^{(0)}(k)} \left(1 - \frac{T_0^{(1)}(k)}{T_0^{(0)}(k)} + \dots \right) \quad (9)$$

reproduce the ERE parameters a_0 , r_0 , P_0 , *etc.* in the inverse of Eq. (1). Then other observables, such as the pole positions, can be predicted. Other renormalization conditions can be imposed instead. For example, one can fit the pole positions, if known, at LO and predict ERE parameters. As long as only low-energy input is used, different renormalization conditions differ only by higher-order effects.

We can obtain the expansion of $T_0(k)$ using Feynman diagrams (see App. A). In this case, we have to calculate loop diagrams which involve the Schrödinger propagator. After renormalization, when positive powers of Λ have been removed from loops, each loop effectively contributes $\mathcal{O}(mk/4\pi)$, while interaction vertices contribute $4\pi C_n k^{2n}/m$. The LO potential has to be iterated to all orders if $C_n^{(0)} = \mathcal{O}(1/M_{l_o}^{n+1})$, since then diagrams involving these vertices form a series in k/M_{l_o} which, once resummed, can give rise to a pole with $|k| \sim M_{l_o}$. The resummation of Feynman diagrams is equivalent to the exact solution of the Schrödinger equation. By definition, higher-order LECs have additional inverse powers of M_{hi} , $C_n^{(N)} = \mathcal{O}(1/M_{l_o}^{n-N+1} M_{hi}^N)$. Subleading interactions are dealt with in distorted-wave perturbation theory, which is equivalent to a finite number of insertions of subleading vertices in Feynman diagrams that include all possible LO vertices. We find the Schrödinger equation easier to implement, especially at subleading orders, and we present explicitly here the calculation of $T_0^{(0,1)}(k)$.

A. Leading order

If the incoming free-particle state with energy $E \equiv k^2/m$ is denoted by $|\vec{k}\rangle$, the scattering amplitude from the LO potential $V^{(0)}$, Eq. (6), is (see, for example, Ref. [2])

$$\begin{aligned} T_0^{(0)}(k) &= \langle \psi_-^{(0)} | \hat{V}^{(0)} | \vec{k} \rangle = \frac{4\pi}{m} \left[\left(C_0^{(0)} + \frac{C_2^{(0)}}{2} k^2 \right) \psi_-^{(0)*}(0) - \frac{C_2^{(0)}}{2} \psi_-^{(0)''*}(0) \right] \\ &= \langle \vec{k} | \hat{V}^{(0)} | \psi_+^{(0)} \rangle = \frac{4\pi}{m} \left[\left(C_0^{(0)} + \frac{C_2^{(0)}}{2} k^2 \right) \psi_+^{(0)}(0) - \frac{C_2^{(0)}}{2} \psi_+^{(0)''}(0) \right], \end{aligned} \quad (10)$$

where $|\psi_+^{(0)}\rangle$ ($|\psi_-^{(0)}\rangle$) is the incoming (outgoing) scattering wavefunction and $\psi'' \equiv \nabla^2 \psi$. The scattering wavefunctions are combinations of homogeneous (free-field) and particular (potential term with free-field Green's function) solutions of the Schrödinger equation,

$$\psi_{\pm}^{(0)}(\vec{r}) = e^{i\vec{k}\cdot\vec{r}} - 4\pi \int \frac{d^3q}{(2\pi)^3} \frac{e^{i\vec{q}\cdot\vec{r}}}{q^2 - k^2 \mp i\epsilon} \left[\left(C_0^{(0)} + \frac{C_2^{(0)}}{2} q^2 \right) \psi_{\pm}^{(0)}(0) - \frac{C_2^{(0)}}{2} \psi_{\pm}^{(0)''}(0) \right]. \quad (11)$$

We define the integrals

$$I_{2n}^{\pm}(k) = -4\pi \int \frac{d^3q}{(2\pi)^3} \frac{q^{2n}}{q^2 - k^2 \mp i\epsilon} = - \sum_{\ell=0}^{\infty} L_{1+2(n-\ell)} k^{2\ell} \mp ik^{2n+1}, \quad (12)$$

where

$$L_{\ell} = \theta_{\ell} \Lambda^{\ell}, \quad (13)$$

with θ_{ℓ} a regulator-dependent number — for example, $\theta_{\ell} = 2/(\ell\pi)$ for a sharp-cutoff regulator. These integrals allow us to write

$$\psi_{\pm}^{(0)}(0) = 1 - \left(C_0^{(0)} \psi_{\pm}^{(0)}(0) - \frac{C_2^{(0)}}{2} \psi_{\pm}^{(0)''}(0) \right) I_0^{\pm}(k) - \frac{C_2^{(0)}}{2} \psi_{\pm}^{(0)}(0) I_2^{\pm}(k), \quad (14)$$

$$\psi_{\pm}^{(0)''}(0) = -k^2 + \left(C_0^{(0)} \psi_{\pm}^{(0)}(0) - \frac{C_2^{(0)}}{2} \psi_{\pm}^{(0)''}(0) \right) I_2^{\pm}(k) - \frac{C_2^{(0)}}{2} \psi_{\pm}^{(0)}(0) I_4^{\pm}(k). \quad (15)$$

Using Eqs. (12), (14) and (15) we solve for $\psi_{\pm}^{(0)}(0)$ and $\psi_{\pm}^{(0)''}(0)$ in terms of $C_{0,2}^{(0)}$, $L_{5,3}(k)$ and $I_0^+(k)$. We have

$$\frac{4\pi}{m T_0^{(0)}(k)} = \frac{1}{v_0^{(0)} + v_2^{(0)} k^2} - I_0^+(k), \quad (16)$$

where

$$v_0^{(0)} = \frac{C_0^{(0)} - C_2^{(0)2} L_5/4}{(1 + C_2^{(0)} L_3/2)^2}, \quad (17)$$

$$v_2^{(0)} = C_2^{(0)} \frac{1 + C_2^{(0)} L_3/4}{(1 + C_2^{(0)} L_3/2)^2}, \quad (18)$$

a result obtained in Refs. [24, 25]. Equation (16) is the same T matrix we would have obtained with an energy-dependent potential $v_0^{(0)} + v_2^{(0)} k^2$. With our momentum-dependent interactions, however, $v_{0,2}^{(0)}$ differ from $C_{0,2}^{(0)}$ by cutoff-dependent factors that trace back to the increased singularity of the two-derivative term.

As it stands, the T matrix (16) depends on the regulator through $I_0^+(k)$, $L_{3,5}$, and $C_{0,2}^{(0)}$. In particular, the linear cutoff dependence of $I_0^+(k)$ needs to be eliminated. Our renormalization procedure involves expanding Eq. (16) in powers of k/Λ and equating it to the ERE in Eq. (1). The unitarity term ik stems from $I_0^+(k)$, and the first two

powers of k^2 allow us to express the bare parameters $C_0^{(0)}(\Lambda)$ and $C_2^{(0)}(\Lambda)$ as functions of the L_n and the observables a_0 and r_0 . Using Eq. (13) (details can be found in App. B), we obtain for $r_0 \neq 0$

$$C_0^{(0)}(\Lambda) = \frac{\theta_5}{\theta_3^2 \Lambda} \left[1 \mp 2\varepsilon + \left(1 - \frac{\theta_3^2}{\theta_5 \theta_1} \right) \varepsilon^2 \pm \left(1 - \frac{\theta_3 \theta_{-1}}{\theta_1^2} - \frac{\theta_3 r_0}{\theta_1^3 a_0} \right) \varepsilon^3 + \mathcal{O} \left(\varepsilon^4, \frac{r_0}{a_0} \varepsilon^4 \right) \right], \quad (19)$$

$$C_2^{(0)}(\Lambda) = -\frac{2}{\theta_3 \Lambda^3} \left[1 \mp \varepsilon \pm \left(1 - \frac{\theta_3 \theta_{-1}}{\theta_1^2} - \frac{\theta_3 r_0}{\theta_1^3 a_0} \right) \frac{\varepsilon^3}{2} + \mathcal{O} \left(\varepsilon^5, \frac{r_0}{a_0} \varepsilon^5 \right) \right], \quad (20)$$

where we introduced

$$\varepsilon = \left(-\frac{2\theta_1^2}{\theta_3 r_0 \Lambda} \right)^{1/2}. \quad (21)$$

There are two solutions indicated by the \pm signs accompanying the unusual inverse powers of $(-r_0 \Lambda)^{1/2}$. For real $C_0^{(0)}$ and $C_2^{(0)}$, we see from Eqs. (19) and (20) that we must have $r_0 < 0$. This result is consistent with the Wigner bound [26], which puts a condition on the rate of change of the phase shift with respect to the energy for a finite-range, energy-independent potential. It translates [33, 34] into a constraint on the effective range r_0 ,

$$r_0 \leq 2R \left(1 - \frac{R}{a_0} + \frac{R^2}{3a_0^2} \right). \quad (22)$$

Interpreting the range R of the potential as the inverse cutoff in momentum space, $R \sim 1/\Lambda$, the limit $\Lambda \rightarrow \infty$ corresponds to a zero-range interaction ($R \rightarrow 0$). In this limit there is no positive effective range consistent with Eq. (22) [25]. The requirement of renormalizability for our LO interactions automatically yields the same constraint.

Now we substitute the expressions for $C_0^{(0)}$ and $C_2^{(0)}$ in terms of the scattering length, the effective range and the cutoff into the expression (16) and expand $T_0^{(0)}(k)$ about $k/\Lambda \rightarrow 0$,

$$T_0^{(0)}(k) = -\frac{4\pi}{m} \left(-\frac{1}{a_0} + \frac{r_0}{2} k^2 - ik \right)^{-1} \left[1 + \left(-\frac{1}{a_0} + \frac{r_0}{2} k^2 - ik \right)^{-1} \frac{r_0^2}{4\theta_1 \Lambda} k^4 + \dots \right] \quad (23)$$

$$= -\frac{4\pi}{m} \left(-\frac{1}{a_0} + \frac{r_0}{2} k^2 - ik + \frac{r_0^2}{4\theta_1 \Lambda} k^4 \right)^{-1} + \dots \quad (24)$$

Because the renormalized $C_0^{(0)}$ and $C_2^{(0)}$ involve only M_{lo} , the ERE parameters scale as $a_0 \sim r_0 \sim 1/M_{lo}$, as needed for a shallow resonance. For $k \sim M_{lo}$, the first three terms in the denominator on the right-hand side of Eq. (24) are $\mathcal{O}(M_{lo})$, while the fourth term can be made arbitrarily small as Λ increases. The first three terms generate two poles, including a resonance, which we discuss in Sec. IV, and give rise to the LO phase shift

$$k \cot \delta_0^{(0)}(k) = -\frac{1}{a_0} + \frac{r_0}{2} k^2. \quad (25)$$

For $\Lambda \gtrsim M_{hi}$, the fourth term is no larger than $\mathcal{O}(M_{lo}^2/M_{hi})$. Barring further fine tuning, this term is comparable to NLO interactions which will remove its residual cutoff dependence. In fact, it can be thought as an induced shape parameter $1/(4\theta_1 r_0 \Lambda)$. Taking $\Lambda \sim M_{hi}$ in

$$\Delta \left(k \cot \delta_0^{(0)}(k) \right) = \frac{r_0^2}{4\theta_1 \Lambda} k^4 \quad (26)$$

gives an estimate of the error in $k \cot \delta_0^{(0)}(k)$. In this case, the right-hand side of Eq. (26) is indeed $\mathcal{O}(M_{lo}/M_{hi})$ relative to Eq. (25).

At this point we have shown, following Refs. [24, 25], that the EFT can produce the first two terms in the ERE at LO, as long as the effective range $r_0 < 0$. In the next section we show how subleading contributions systematically improve the LO result.

B. Subleading order

Adding perturbations to the LO implies that the corresponding changes in the scattering amplitude should be treated in (distorted-wave) perturbation theory. The first correction to the T matrix, $T_0^{(1)}(k)$, is linear in the parameters of

the NLO potential, the $C_{0,2,4}^{(1)}$ defined in Eq. (5). After renormalization, $C_4^{(1)} = \mathcal{O}(1/M_{lo}^4 M_{hi})$ since its contribution must be comparable to the LO error in Eq. (26). And, since they are of the same order, $C_0^{(1)} = \mathcal{O}(1/M_{hi})$ and $C_2^{(1)} = \mathcal{O}(1/M_{lo}^2 M_{hi})$.

Explicitly (see Ref. [2] again),

$$\begin{aligned} T_0^{(1)}(k) &= \langle \psi_-^{(0)} | V^{(1)} | \psi_+^{(0)} \rangle = \langle \psi_+^{(0)} | V^{(1)} | \psi_-^{(0)} \rangle \\ &= \frac{4\pi}{m} \left[C_0^{(1)} \psi_-^{(0)*}(0) \psi_+^{(0)}(0) - C_2^{(1)} \psi_-^{(0)*}(0) \psi_+^{(0)''}(0) + \frac{C_4^{(1)}}{2} \left(\psi_-^{(0)*}(0) \psi_+^{(0)''''}(0) + \psi_-^{(0)*''}(0) \psi_+^{(0)''}(0) \right) \right], \end{aligned} \quad (27)$$

where $\psi_+^{(0)''''} \equiv \nabla^4 \psi_+^{(0)}$ is given by

$$\psi_{\pm}^{(0)''''}(0) = k^4 - \left(C_0^{(0)} \psi_{\pm}^{(0)}(0) - \frac{C_2^{(0)}}{2} \psi_{\pm}^{(0)''}(0) \right) I_4^{\pm}(k) - \frac{C_2^{(0)}}{2} \psi_{\pm}^{(0)}(0) I_6^{\pm}(k). \quad (28)$$

Once this is substituted in Eq. (27),

$$\frac{T_0^{(1)}(k)}{T_0^{(0)2}(k)} = \frac{m}{4\pi} \frac{v_0^{(1)} + v_2^{(1)} k^2 + v_4^{(1)} k^4}{(v_0^{(0)} + v_2^{(0)} k^2)^2}, \quad (29)$$

where

$$\begin{aligned} v_0^{(1)} &= \frac{1}{(1 + C_2^{(0)} L_3/2)^2} \left\{ C_0^{(1)} - C_2^{(1)} \frac{C_0^{(0)} L_3 + C_2^{(0)} L_5/2}{1 + C_2^{(0)} L_3/2} + \frac{C_4^{(1)}/2}{(1 + C_2^{(0)} L_3/2)^2} \left[C_0^{(0)} L_3 (C_0^{(0)} L_3 + C_2^{(0)} L_5/2) \right. \right. \\ &\quad \left. \left. - C_0^{(0)} L_5 + C_2^{(0)2} (1 + C_2^{(0)} L_3/4) (L_5^2 - L_3 L_7)/2 - C_2^{(0)} L_7/2 \right] \right\}, \end{aligned} \quad (30)$$

$$v_2^{(1)} = \frac{1}{(1 + C_2^{(0)} L_3/2)^3} \left[C_2^{(1)} - \frac{C_4^{(1)}}{2} \left(C_0^{(0)} L_3 + C_2^{(0)} L_5 + 2 \frac{C_0^{(0)} L_3 + C_2^{(0)} L_5/2}{1 + C_2^{(0)} L_3/2} \right) \right], \quad (31)$$

$$v_4^{(1)} = C_4^{(1)} \frac{1 + C_2^{(0)} L_3/4}{(1 + C_2^{(0)} L_3/2)^4}. \quad (32)$$

Again, Eq. (29) is the result we would obtain by treating an energy-dependent potential $v_0^{(1)} + v_2^{(1)} k^2 + v_4^{(1)} k^4$ in first-order perturbation theory. In our case, however, the additional singularity of two- and four-derivative interactions leads to the relations (30), (31), and (32).

As before, we renormalize the NLO amplitude by expanding the right-hand side of Eq. (9) in powers of k/Λ and matching it to the ERE, Eq. (1). The presence of $C_4^{(1)} = \mathcal{O}(1/M_{lo}^4 M_{hi})$ now ensures that the quartic power of momentum can be made cutoff-independent by demanding that it reproduce the empirical value of the shape parameter P_0 . The other two NLO parameters, $C_{0,2}^{(1)}$, can be chosen so that the terms independent of and quadratic in momentum remain unchanged. Again, with details given in App. B, we find

$$\begin{aligned} C_0^{(1)}(\Lambda) &= \frac{\theta_1^2}{2\theta_3^4} (\theta_7 \theta_3 - 2\theta_5^2) P_0 r_0 \left\{ 1 - \left[2 - \frac{\theta_5(\theta_5 \theta_1 - 2\theta_3^2)}{\theta_1(\theta_7 \theta_3 - 2\theta_5^2)} \right] \varepsilon - \left[\frac{\theta_5^2 \theta_1^2 - 3\theta_5 \theta_3^2 \theta_1 + \theta_3^4}{\theta_1^2 (\theta_7 \theta_3 - 2\theta_5^2)} - \frac{2\theta_3 \theta_{-1}}{\theta_1^2} - \frac{\theta_3 r_0}{\theta_1^3 a_0} \right] \varepsilon^2 \right. \\ &\quad \left. + \mathcal{O} \left(\varepsilon^3, \frac{r_0}{a_0} \varepsilon^3 \right) \right\} + \frac{\theta_1}{\theta_3^4 \Lambda} (\theta_7 \theta_3 - 2\theta_5^2) [1 + \mathcal{O}(\varepsilon)], \end{aligned} \quad (33)$$

$$\begin{aligned} C_2^{(1)}(\Lambda) &= \frac{3\theta_5 \theta_1^2}{2\theta_3^3} \frac{P_0 r_0}{\Lambda^2} \left[1 - \left(5 - \frac{2\theta_3^2}{\theta_5 \theta_1} \right) \frac{\varepsilon}{3} - \left(\frac{2}{3} + \frac{\theta_3^2}{3\theta_1 \theta_5} - \frac{2\theta_3 \theta_{-1}}{\theta_1^2} - \frac{\theta_3 r_0}{\theta_1^3 a_0} \right) \varepsilon^2 + \mathcal{O} \left(\varepsilon^3, \frac{r_0}{a_0} \varepsilon^3 \right) \right] \\ &\quad + \frac{3\theta_5 \theta_1}{\theta_3^3 \Lambda^3} [1 + \mathcal{O}(\varepsilon)], \end{aligned} \quad (34)$$

$$C_4^{(1)}(\Lambda) = -\frac{\theta_1^2}{\theta_3^2} \frac{P_0 r_0}{\Lambda^4} \left[1 - \varepsilon - \left(1 - \frac{2\theta_3 \theta_{-1}}{\theta_1^2} - \frac{\theta_3 r_0}{\theta_1^3 a_0} \right) \varepsilon^2 + \mathcal{O} \left(\varepsilon^3, \frac{r_0}{a_0} \varepsilon^3 \right) \right] - \frac{2\theta_1}{\theta_3^2 \Lambda^5} [1 + \mathcal{O}(\varepsilon)]. \quad (35)$$

The terms independent of P_0 are those induced by the residual cutoff dependence in the quartic term of Eq. (24). The others are all linear in the NLO physical parameter P_0 , whose sign is not constrained by renormalization at this order. The situation here is analogous to the one-pole case [9–12], where the perturbative treatment of C_2 places no renormalization constraints on the sign of r_0 .

At this point we have tuned C_0 , C_2 and C_4 in such a way that they reproduce the ERE in Eq. (1) exactly in the limit $\Lambda \rightarrow \infty$. For a large but finite Λ , the NLO EFT reproduces Eq. (1) up to a correction that goes as the sixth power of momentum,

$$T_0^{(0+1)}(k) = -\frac{4\pi}{m} \left[-\frac{1}{a_0} + \frac{r_0}{2}k^2 - P_0 \left(\frac{r_0}{2}\right)^3 k^4 - ik - \frac{P_0 r_0^4}{8\theta_1 \Lambda} k^6 \right]^{-1} + \dots \quad (36)$$

Because $C_4 = \mathcal{O}(1/M_{l_0}^4 M_{hi})$, here the shape parameter $P_0 = \mathcal{O}(M_{l_0}/M_{hi})$. The phase shift up to NLO is given by

$$k \cot \delta_0^{(0+1)}(k) = -\frac{1}{a_0} + \frac{r_0}{2}k^2 - P_0 \left(\frac{r_0}{2}\right)^3 k^4, \quad (37)$$

with an error that can be estimated from the k^6 term once we take $\Lambda \rightarrow M_{hi}$ in

$$\Delta \left(k \cot \delta_0^{(0+1)}(k) \right) = \frac{|P_0| r_0^4}{8|\theta_1| \Lambda} k^6. \quad (38)$$

This error shows that at N²LO a $(\psi^\dagger \psi)(\psi^\dagger \overleftrightarrow{\nabla}^6 \psi)$ interaction with LEC $4\pi C_6/m$ is needed, where after renormalization $C_6 = \mathcal{O}(1/M_{l_0}^5 M_{hi}^2)$. At this order this interaction is solved in first-order distorted-wave perturbation theory, while NLO interactions need to be accounted for in second order. The procedure continues at higher orders in an obvious way.

IV. POLES AND RESIDUES

The distinctive feature of our LO is the existence of two S -wave S -matrix poles, allowing for the possibility of a resonance. Our S -wave S matrix can be written as

$$S_0(k) = 1 - \frac{imk}{2\pi} T_0(k) = e^{2i\phi(k)} \frac{(k+k_1)(k+k_2)}{(k-k_1)(k-k_2)}, \quad (39)$$

where $k_{1,2} \neq 0$ denote the pole positions and $\phi(k)$ is the nonresonant or “background” contribution to the phase shift. These quantities can be expanded order by order, and we now obtain them up to NLO.

A. Leading order

The S matrix corresponding the LO T matrix (24), $S_0^{(0)}(k)$, is nothing but that corresponding to the effective-range approximation to the ERE, that is, Eq. (39) with [35]

$$k_{1,2}^{(0)} = \frac{1}{r_0} \left(i \pm \sqrt{\frac{2r_0}{a_0} - 1} \right) \quad (40)$$

and

$$\phi^{(0)}(k) = 0. \quad (41)$$

While the effective range $r_0 < 0$ for renormalization, the scattering length a_0 can be positive or negative, giving rise to five qualitatively distinct cases:

1. $-2|r_0| < a_0 < 0$: there are two resonance poles

$$k_1^{(0)} = k_R - ik_I, \quad (42)$$

$$k_2^{(0)} = -k_R - ik_I, \quad (43)$$

with

$$k_I = \frac{1}{|r_0|} > 0, \quad (44)$$

$$k_R = \frac{1}{|r_0|} \sqrt{\frac{2r_0}{a_0} - 1} > 0. \quad (45)$$

The two poles are thus forced to be in the lower half of the complex momentum plane by the requirement of renormalizability. This is in agreement with the general requirement on the S matrix [1, 36, 37] that leads to states decaying with time. In the limit $\Lambda \rightarrow \infty$ we obtain the well-known form

$$S_0^{(0)}(E) = \frac{E - E_0^{(0)} - i\Gamma^{(0)}(E)/2}{E - E_0^{(0)} + i\Gamma^{(0)}(E)/2}, \quad (46)$$

where

$$E_0^{(0)} = \frac{k_R^2 + k_I^2}{m} = \frac{2}{ma_0 r_0} > 0, \quad (47)$$

$$\Gamma^{(0)}(E) = \frac{4kk_I}{m} = \frac{4}{m|r_0|} \sqrt{mE} > 0. \quad (48)$$

The residues of $iS_0^{(0)}$ at the poles are complex,

$$\text{Res}\left(iS_0^{(0)}\right)\Big|_{\pm k_R - ik_I} = 2k_I \left(1 \mp i \frac{k_I}{k_R}\right). \quad (49)$$

Our power counting describes the situation $|a_0| \sim |r_0| \sim 1/M_{lo}$, where the resonance is shallow but broad in the sense that $k_I \sim k_R \sim M_{lo} \ll M_{hi}$. We cannot exclude a situation where $r_0 \gg a_0$ and the resonance is narrow, that is, $k_R \gg k_I$ with nearly real and positive residues [35]. However, our power counting is somewhat artificial in this case, since the unitarity term $-ik$ in Eq. (24) is small compared to the inverse scattering length and the effective range, except near the pole. A narrow resonance arises more naturally from a dimeron field where residual mass and kinetic terms are treated as LO, while loops are included perturbatively except in the vicinity of the resonance [15].

2. $a_0 = -2|r_0|$: there is a double pole on the negative imaginary axis [38],

$$k_1^{(0)} = k_2^{(0)} \equiv k_{1\equiv 2} = -\frac{i}{|r_0|}, \quad (50)$$

with positive residue

$$\text{Res}\left(iS_0^{(0)}\right)\Big|_{k_{1\equiv 2}} = 4ik_{1\equiv 2} > 0. \quad (51)$$

This represents a virtual state. A double pole on the upper plane is again excluded by the requirement of renormalizability, in agreement with other arguments [1, 36, 38].

3. $a_0 < -2|r_0|$: there are two virtual states represented by poles on the negative imaginary axis,

$$k_1^{(0)} = -i\kappa_-, \quad (52)$$

$$k_2^{(0)} = -i\kappa_+, \quad (53)$$

where

$$\kappa_{\pm} = \frac{1}{|r_0|} \left(1 \pm \sqrt{1 - \frac{2r_0}{a_0}}\right) > 0. \quad (54)$$

They have residues of opposite signs,

$$\text{Res}\left(iS_0^{(0)}\right)\Big|_{-i\kappa_{\pm}} = \pm 2\kappa_{\pm} \frac{\kappa_+ + \kappa_-}{\kappa_+ - \kappa_-}, \quad (55)$$

the shallowest pole (k_1) with the negative sign.

a_0, r_0	- , -	+ , -	- , +	+ , +
$\text{Im } k_1, \text{Im } k_2$	- , -	+ , -	- , +	+ , +
$\text{Res}(iS_0^{(0)}) _{k_1}, \text{Res}(iS_0^{(0)}) _{k_2}$	- , +	+ , +	- , -	+ , -
pole 1, pole 2	V, V	B, V	V, R	B, R

TABLE I: Character of (simple) poles on the imaginary axis according to the signs of the scattering length a_0 and effective range r_0 for $|\text{Im } k_2| > |\text{Im } k_1|$. In the last row V stands for virtual state, B for bound state, and R for redundant pole. Only the first two columns are allowed by renormalization of the EFT.

4. $a_0 > 0$: the two poles are on opposite sides of the imaginary axis,

$$k_1^{(0)} = i\kappa_-, \quad (56)$$

$$k_2^{(0)} = -i\kappa_+, \quad (57)$$

where

$$\kappa_{\pm} = \frac{1}{|r_0|} \left(\sqrt{1 + \frac{2|r_0|}{a_0}} \pm 1 \right) > 0. \quad (58)$$

Both residues are positive,

$$\text{Res}\left(iS_0^{(0)}\right)\Big|_{\mp i\kappa_{\pm}} = 2\kappa_{\pm} \frac{\kappa_+ - \kappa_-}{\kappa_+ + \kappa_-} > 0. \quad (59)$$

This indicates that the pole k_1 on the positive imaginary axis is a bound state [1]. The constraint $r_0 < 0$ from renormalization thus excludes the possibility of a “redundant” pole [39–41] on the positive imaginary axis with negative residue. If the effective range were positive, such a pole could arise together with a shallower bound or virtual state for, respectively, $a_0 > 2r_0$ or $a_0 < 0$, see Table I. The interpretation of a redundant pole is unclear: it has a non-normalizable wavefunction [40, 42], but carries information about the asymptotic behavior of continuum states [43]. Since at least in a nonrelativistic setting its position is determined by the range of the potential [35, 44, 45], it is comforting that renormalization of our EFT prevents a shallow redundant pole.

5. $|a_0|^{-1} = 0$: this is the boundary between the previous two cases. It is essentially the limit $|a_0| \rightarrow \infty$ of these cases, except that the S matrix has a single pole

$$k_2^{(0)} = -i\kappa_+ = -2i|r_0|, \quad (60)$$

with positive residue

$$\text{Res}\left(iS_0^{(0)}\right)\Big|_{-i\kappa_+} = 2\kappa_+ > 0. \quad (61)$$

The other, would-be S -matrix pole is only a pole of the T matrix which is sometimes called a zero-energy resonance. When $|r_0| \sim 1/M_{hi}$, the corresponding EFT [9–12] is scale invariant at LO with no other low-energy T -matrix pole. Here, the dimensionful parameter $|r_0| \sim 1/M_{lo}$ explicitly breaks scale invariance at LO, generating a virtual pole.

When we use effective-range parameters to fix the LECs, the pole positions have an uncertainty $\Delta k^{(0)}$ due to the neglect of higher orders. We can estimate the magnitude of the error from the residual cutoff dependence in Eq. (24) and then varying the cutoff from the theory’s breakdown scale to much larger values. We find

$$|\Delta k_{1,2}^{(0)}| = \frac{r_0^2}{4\Lambda} \left| \frac{k_{1,2}^{(0)4}}{\theta_1 \sqrt{\frac{2r_0}{a_0} - 1}} \right|, \quad a_0 \neq 2r_0, \quad (62)$$

$$= \frac{1}{|r_0|} \sqrt{\frac{1}{2|\theta_1 r_0| \Lambda}}, \quad a_0 = 2r_0, \quad (63)$$

with $\Lambda \sim M_{hi}$. Evidently $\Delta k^{(0)} = 0$ if we use the pole positions as input.

B. Subleading order

If their positions are not used as input, the pole positions will move slightly at subleading orders and approach, if the theory is converging, their exact locations. As before, the procedure is systematic and we illustrate it only for NLO.

When both poles are simple, that is, for $a_0 \neq 2r_0$, the pole positions can be written as

$$k_{1,2}^{(0+1)} = k_{1,2}^{(0)} + k_{1,2}^{(1)} \quad (64)$$

in terms of the NLO shift

$$k_{1,2}^{(1)} = \frac{P_0}{|r_0|} \left[\mp \frac{1}{\sqrt{\frac{2r_0}{a_0} - 1}} \left(\frac{r_0^2}{2a_0^2} - \frac{2r_0}{a_0} + 1 \right) + i \left(1 - \frac{r_0}{a_0} \right) \right]. \quad (65)$$

This is precisely what is needed to cancel the spurious double pole in $T_0^{(1)}$ (the ‘‘good-fit condition’’ of Ref. [46]). Now the error is reduced to the size of N²LO interactions when Λ is above the breakdown scale of the theory,

$$|\Delta k_{1,2}^{(1)}| = \frac{r_0^4}{8\Lambda} \left| \frac{P_0 k_{1,2}^{(0)6}}{\theta_1 \sqrt{\frac{2r_0}{a_0} - 1}} \right|. \quad (66)$$

In contrast, when $a_0 = 2r_0$ the double nature of the pole leads to an expansion in half powers for its position,

$$k_{1,2}^{(0+1)} = k_{1\equiv 2}^{(0)} + k_{1,2}^{(1/2)} + k_{1\equiv 2}^{(1)}, \quad (67)$$

where

$$k_{1,2}^{(1/2)} = \pm \frac{\sqrt{P_0}}{2|r_0|}, \quad (68)$$

$$k_{1\equiv 2}^{(1)} = i \frac{P_0}{2|r_0|}. \quad (69)$$

We will refer to the half-power correction as N^{1/2}LO. While the smaller NLO correction is imaginary, the N^{1/2}LO correction is real for $P_0 > 0$, indicating that in the underlying theory the resonant poles have not coalesced. Conversely, $P_0 < 0$ would imply the underlying poles are already two separated virtual states. There is no separate Λ -dependent error estimate for the N^{1/2}LO displacement. As an estimate for the error we take

$$|\Delta k_{1,2}^{(1/2)}| = \frac{|P_0|}{2|r_0|}, \quad (70)$$

which is $\sqrt{P_0} \sim \mathcal{O}((M_{lo}/M_{hi})^{1/2})$ smaller than $k_{1,2}^{(1/2)}$ in Eq. (68). This estimate could easily be off by a factor of $\mathcal{O}(1)$, but it accidentally exactly coincides with the magnitude of the NLO shift (69). The Λ -dependent error of the latter scales as the 3/2 power of the expansion parameter,

$$|\Delta k_{1,2}^{(1)}| = \frac{\sqrt{|P_0|}}{4r_0^2|\theta_1|\Lambda}. \quad (71)$$

In either case, up to higher-order terms the NLO S matrix $S_0^{(0+1)}(k)$ is given by Eq. (39) but with the poles at their NLO positions $k_{1,2}^{(0+1)}$ and

$$\phi^{(0+1)}(k) = \frac{P_0 r_0}{2} k \equiv -c k. \quad (72)$$

The nonresonant contribution to the phase shift is a subleading effect linear in k . This form of the S matrix for short-range forces with two poles has been arrived at by causality-type arguments [36, 47], with $c \geq 0$ related to the range R of the force. For $c \geq 0$ we have $P_0 \geq 0$, although this constraint does not follow from renormalization of our EFT to NLO.

As we have seen, the renormalization condition on the EFT allows only the standard cases of a (decaying) resonance, a bound state, and virtual states. The pole positions can be determined from the effective-range parameters with increasing precision as the order increases. In order to show explicitly that the accuracy also improves, we consider an explicit example of underlying theory next.

V. TOY MODEL

The inclusion of all interactions allowed by symmetries ensures that any underlying dynamics producing the same low-energy pole structure can be accommodated in the EFT. Information about the dynamics at short-distance scales is encoded in the LECs. We now consider a simple model for the short-distance physics, in order to illustrate how the EFT captures the long-distance dynamics associated to the existence of two shallow poles.

As a toy model we take a potential consisting of an attractive spherical well of range R and depth β^2/mR^2 with a repulsive delta shell with strength α/mR at its edge:

$$V(r) = \frac{\alpha}{mR} \delta(r - R) - \frac{\beta^2}{mR^2} \theta(R - r), \quad (73)$$

with $\alpha > 0$ and $\beta > 0$. This model was used for resonances in Ref. [17]. The Schrödinger equation is easily solved in the S -wave in the standard fashion inside ($r < R$) and outside ($r > R$), with the wavefunctions and their derivatives matched at the range R . One finds

$$\cot \delta_0(k) = -\frac{\kappa R \cot(\kappa R) \cot(kR) + \alpha \cot(kR) + kR}{\kappa R \cot(\kappa R) + \alpha - kR \cot(kR)}, \quad (74)$$

where $\kappa = \sqrt{k^2 + \beta^2/R^2}$. Equivalently, the phase shift is given by

$$\delta_0(k) = -kR + \arctan\left(\frac{kR}{\kappa R \cot(\kappa R) + \alpha}\right). \quad (75)$$

A. Scattering length, effective range, and pole positions

We are interested in the dynamics for $k \ll R^{-1} \equiv M_{hi}$. Equations (74) and (75) reduce to the well-known expressions for the attractive spherical well [1] when $\alpha = 0$. In this case there is a single low-energy pole, either a bound or a virtual state, which is captured by the EFT where LO consists of only C_0 and NLO of C_2 [9–12]. For $\alpha > 0$, we can have two low-energy poles. Tuning α and β yields the various cases (bound, virtual, resonant) considered above.

Expanding the inverse of the T matrix in $kR \ll 1$ and matching to the ERE,

$$\frac{a_0}{R} = 1 - \frac{1}{\alpha + \beta \cot \beta}, \quad (76)$$

$$\frac{r_0}{R} = \frac{2(\alpha + \beta \cot \beta)(\alpha + \beta \cot \beta - 3) - 3[\cot^2 \beta - (\cot \beta)/\beta - 1]}{3(\alpha + \beta \cot \beta - 1)^2} \quad (77)$$

$$= 1 - \frac{1}{3} \left(\frac{R}{a_0}\right)^2 - \frac{R}{\beta^2 a_0} - \frac{\alpha}{\beta^2} \left[\alpha + 1 - 2\alpha \frac{R}{a_0} + (\alpha - 1) \left(\frac{R}{a_0}\right)^2 \right]. \quad (78)$$

The next term in the expansion of $T_0^{-1}(k)$ gives an expression for the shape parameter P_0 as a function of the parameters α and β . We plot a_0 and r_0 as functions of β for various values of α in Fig. 1. For most values of the potential parameters, $a_0 \approx R$ and $r_0 \approx R$ as expected from dimensional analysis. Only some specific regions have unnaturally large magnitudes. In the regions where $|a_0| \gg R$, a_0 can be positive or negative, but it is still very likely that $r_0 \approx R$. This is the situation previously investigated in EFT where only C_0 is enhanced. Only in narrow parameter ranges where $\beta \cot \beta \approx -\alpha \ll -1$ can we have both $|a_0| \gg R$ and $|r_0| \gg R$. For a pure spherical well ($\alpha = 0$), r_0/R is given by the first three terms in Eq. (78) and it is easy to see that $|a_0| \gg R$ leads to $r_0 \approx R$. The additional parameter $\alpha > 0$ allows $|r_0| \gg R$. But in this case $r_0 < 0$, just as obtained from renormalization of the EFT considered here, where also C_2 is enhanced.

For given values of a_0 and r_0 , we can solve Eqs. (76) and (77) for α and β , and then use the exact expression for $k \cot \delta_0$ in Eq. (74) to find the poles of T_0 . In the regions where $|a_0|/R \gg 1$ and $|r_0|/R \gg 1$ there are two low-energy poles. An example is shown in Fig. 2 where we hold the strength of the delta shell fixed at $\alpha = 4.68144$ and slightly vary the depth of the well around $\beta^2 \approx 7$. In the plot we begin with $\beta^2 = 6.69$, which gives us two resonance poles, and increase β^2 , which corresponds to increasing the attraction of the well. The two poles collide on the negative imaginary axis creating a double pole, and then one pole moves down as a virtual state while the other moves up until it eventually becomes a bound state. We continue following the increase in binding till $\beta^2 = 7.06$. The pole evolution covers the situations we considered in the previous section. Note that a similar pole evolution exists for the spherical

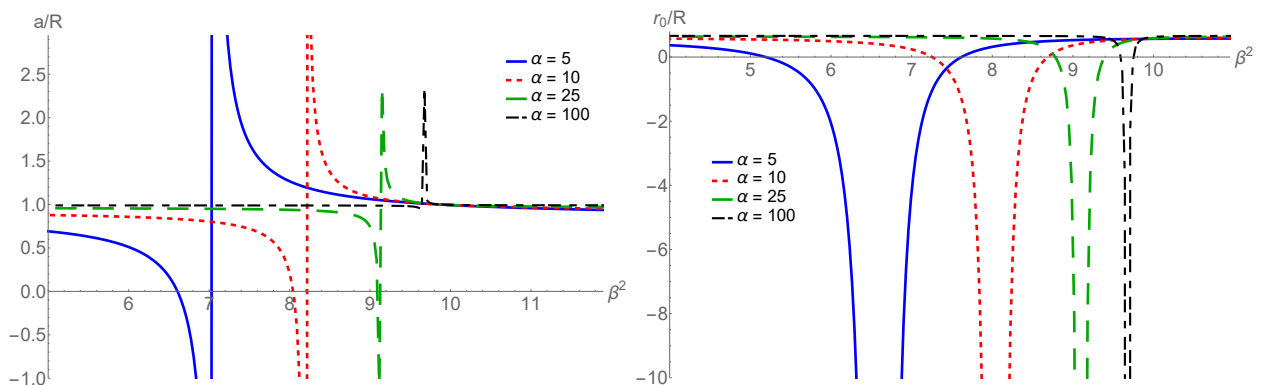


FIG. 1: Scattering length a_0 (left panel) and effective range r_0 (right panel) in units of the potential range R as functions of the square of the strength β of the spherical well, for various values of the strength α of the delta shell.

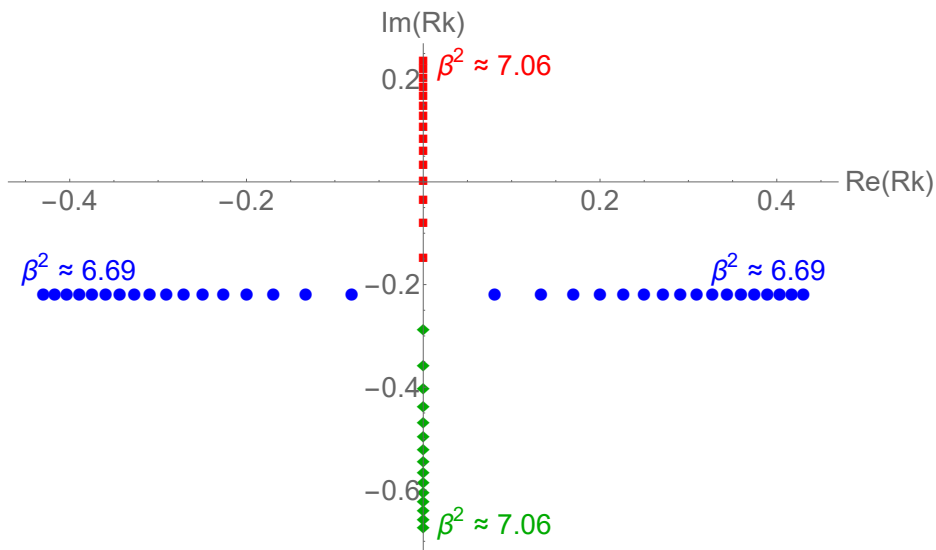


FIG. 2: Pole positions in the kR complex plane for a given strength of the delta-shell potential, $\alpha = 4.68144$. As the depth β^2 of the spherical well increases from 6.69 to 7.06, the two resonance poles (blue circles) approach the imaginary axis and then turn into two virtual poles: one that remains a virtual state (green diamonds), another that eventually becomes a bound state (red squares).

well alone ($\alpha = 0$) [48], but in the latter case the coalescence on the imaginary axis happens at $k_1 = k_2 = -i/R$, which is outside the EFT range. The possibility of this evolution for a general potential well surrounded by a barrier was studied in Ref. [38]. We now turn to a quantitative comparison with the EFT.

B. Comparison with the EFT

We now compare the predictions of the EFT at LO and NLO, using a sharp-cutoff regulator, with the toy model. We choose values for a_0 and r_0 , from which we extract β^2 and α , and calculate P_0 . We fit the EFT to these ERE parameters and compare the resulting phase shifts and pole positions. Since the phase shift is very sensitive to changes in momentum k and there are periodic discontinuities in its derivatives, it is better to work with $k \cot \delta_0$ instead of δ_0 itself. For the toy model we evaluate $k \cot \delta_0$ from Eq. (74). For the EFT we use Eq. (25) at LO and Eq. (37) at NLO, with their corresponding errors in Eqs. (26) and (38). We also compare the position of the poles determined numerically in the toy model with the EFT predictions and their errors given in Sec. IV.

For illustration, we keep the effective range fixed at $r_0/R = -8$ and vary a_0/R so as to reproduce the various cases discussed in the previous section. We start with $a_0/R = -10 > 2r_0/R$. The toy-model parameters for this choice are $\beta^2 = 7.66264$ and $\alpha = 7.15555$, which lead to $P_0 = 0.256439$. On the left panel of Fig. 3 we show the EFT phase

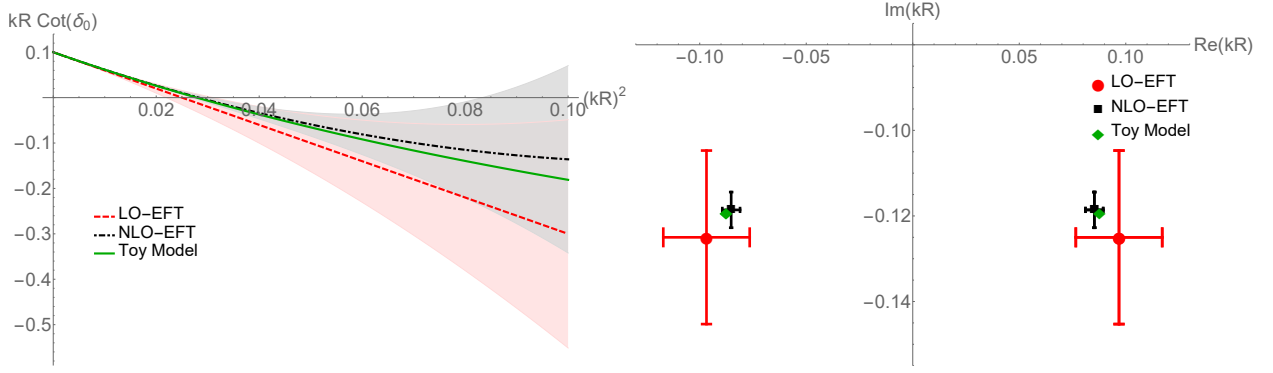


FIG. 3: Comparison between EFT and toy model for $kR \cot \delta_0$ as a function of $(kR)^2$ (left panel) and resonance pole positions on the complex kR plane (right panel), when $\alpha = 7.1555$ and $\beta^2 = 7.66264$. On the left panel, the results for the EFT at LO and NLO are indicated by, respectively, a (red) band around the (red) dashed line and a (gray) band around the (black) dot-dashed line, while the toy model gives the (green) solid line. On the right panel, the EFT at LO and NLO give, respectively, the points with the larger (red) and smaller (black) error bars around the (green) point from the toy model.

	$k_1 R$	$k_2 R$
LO EFT	$(0.10 \pm 0.02) - (0.13 \pm 0.02) i$	$-(0.10 \pm 0.02) - (0.13 \pm 0.02) i$
NLO EFT	$(0.085 \pm 0.004) - (0.119 \pm 0.004) i$	$-(0.085 \pm 0.004) - (0.119 \pm 0.004) i$
Toy model	$0.087583 - 0.119238 i$	$-0.087583 - 0.119238 i$

TABLE II: Position of resonance poles $k_{1,2}$ in units of R^{-1} , when $\alpha = 7.1555$ and $\beta^2 = 7.66264$. The EFT at LO and NLO is compared with the toy model.

shifts at LO and NLO compared to the toy-model values. As expected, the LO EFT agrees with the toy model within an error that increases with energy. The NLO perturbation improves the agreement for the central value and the error is decreased compared to LO. For this choice of parameters the EFT has two resonance poles, just as the toy model. The pole positions are shown on the right panel of Fig. 3 and given in Table II. Again the EFT error bars decrease with order and central values approach the exact result. This example demonstrates the power of EFT to approximate in a systematic and controlled way the T matrix for resonant states.

We now increase the attraction so that $a_0/R = -16 = 2r_0/R$, when the toy-model parameters are $\beta^2 = 7.7321$ and $\alpha = 7.4254$. In this case $P_0 = 0.264856$. The corresponding phase shifts are given on the left panel of Fig. 4. The larger magnitude of the scattering length means $k \cot \delta_0(k)$ is smaller at $k = 0$, but the similar values of toy-model parameters lead to low-energy phase shifts that are not very different from the previous case. The pole positions are given on the right panel of Fig. 4 and in Table III. The increased attraction brings the toy-model poles closer to the imaginary axis. The EFT has a double pole at LO with error bars that encompass the two resonance poles. The half-power correction corrects for the horizontal splitting, and the full NLO correction moves the poles slightly upwards. The convergence pattern is clear, although the NLO error bars are underestimated by a factor of about 2. Had we estimated them by simply multiplying Eq. (69) with $\sqrt{P_0}$, similarly to what we have done at $N^{1/2}$ LO, the NLO error would be about four times larger.

Further increase of the attraction moves the two toy-model poles onto the negative imaginary axis, that is, it creates two virtual states. Taking $a_0/R = -20 < 2r_0/R$, the values for the potential parameters are $\beta^2 = 7.75532$ and $\alpha = 7.51962$, with the shape parameter being $P_0 = 0.267795$. The phase shifts at low energies are seen on the

	$k_1 R$	$k_2 R$
LO EFT	$-(0.13 \pm 0.04) i$	$-(0.13 \pm 0.04) i$
$N^{1/2}$ LO EFT	$(0.03 \pm 0.02) - (0.13 \pm 0.02) i$	$-(0.03 \pm 0.02) - (0.13 \pm 0.02) i$
NLO EFT	$(0.032 \pm 0.003) - (0.108 \pm 0.003) i$	$-(0.032 \pm 0.003) - (0.108 \pm 0.003) i$
Toy model	$0.025286 - 0.112685 i$	$-0.025286 - 0.112685 i$

TABLE III: Position of resonance poles $k_{1,2}$ in units of R^{-1} , when $\alpha = 7.4254$ and $\beta^2 = 7.7321$. The EFT at LO, $N^{1/2}$ LO, and NLO is compared with the toy model.

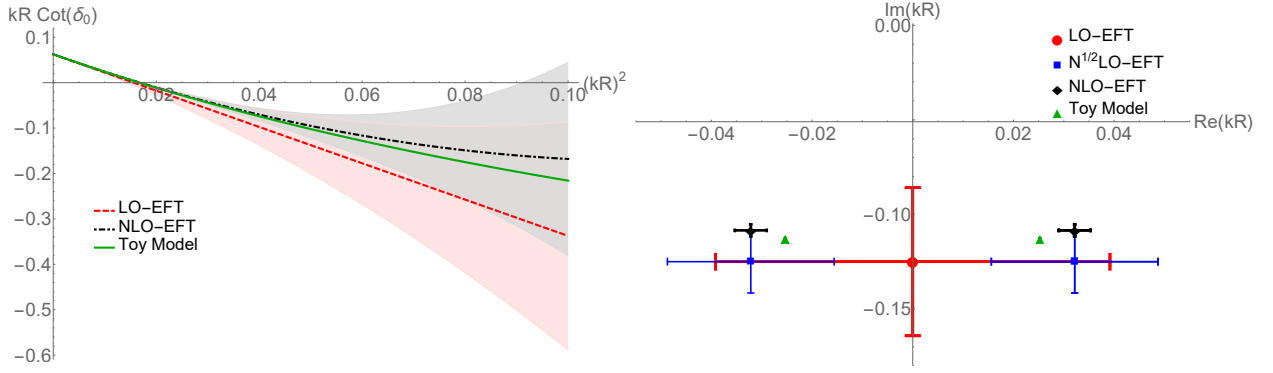


FIG. 4: Comparison between EFT and toy model for $kR \cot \delta_0$ as a function of $(kR)^2$ (left panel) and pole positions on the complex kR plane (right panel), when $\alpha = 7.4254$ and $\beta^2 = 7.7321$. On the right panel, the EFT at N^{1/2}LO gives the (blue) point with intermediate-size error bar. Other notation as in Fig. 3.

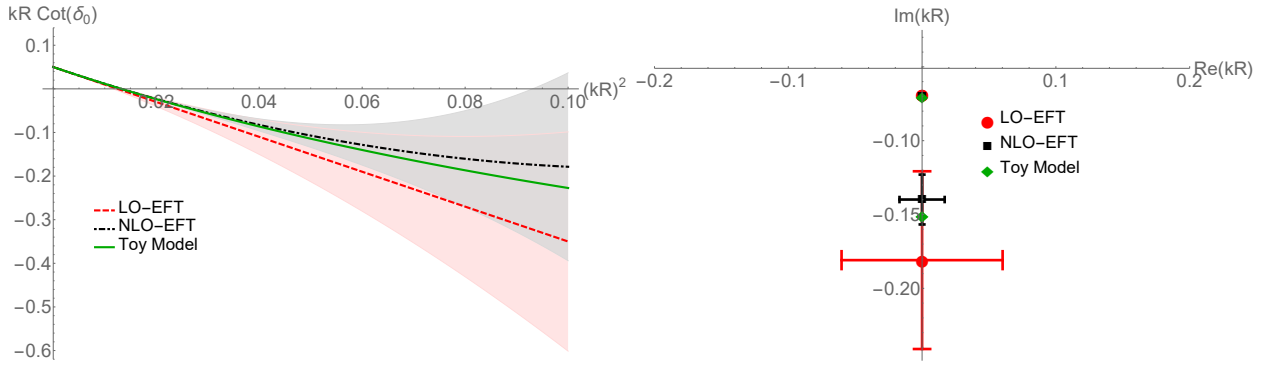


FIG. 5: Comparison between EFT and toy model for $kR \cot \delta_0$ as a function of $(kR)^2$ (left panel) and virtual-state pole positions on the complex kR plane (right panel), when $\alpha = 7.51962$ and $\beta^2 = 7.75532$. Notation as in Fig. 3.

left panel of Fig. 5 to be, again, very similar to the previous cases. The pole positions are nevertheless very different, as shown on the right panel and in Table IV. As expected, the EFT describes the shallower pole very well, but has much larger errors for the deeper state.

Finally, as an example of $a_0/R > 0$, we take $a_0/R = 40$, which translates into $\beta^2 = 7.89592$, $\alpha = 8.13476$, and $P_0 = 0.287009$. The phase shifts continues to resemble earlier cases, except that $a_0 > 0$ changes the sign of the zero-energy value — see the left panel of Fig. 6. The poles are shown on the right panel of Fig. 6 and in Table V. Now there is a shallow bound state for which the EFT converges quickly. The deeper, virtual state has even larger error bars than in the previous example.

These examples are sufficient to illustrate how in all two-pole configurations the EFT reproduces the toy-model results with increased accuracy as the order increases.

	$k_1 R$	$k_2 R$
LO EFT	$-(0.069 \pm 0.001) i$	$-(0.18 \pm 0.06) i$
NLO EFT	$-(0.0700 \pm 0.0001) i$	$-(0.14 \pm 0.02) i$
Toy model	$-0.070047 i$	$-0.150999 i$

TABLE IV: Position of virtual poles $k_{1,2}$ in units of R^{-1} , when $\alpha = 7.51962$ and $\beta^2 = 7.75532$. The EFT at LO and NLO is compared with the toy model.

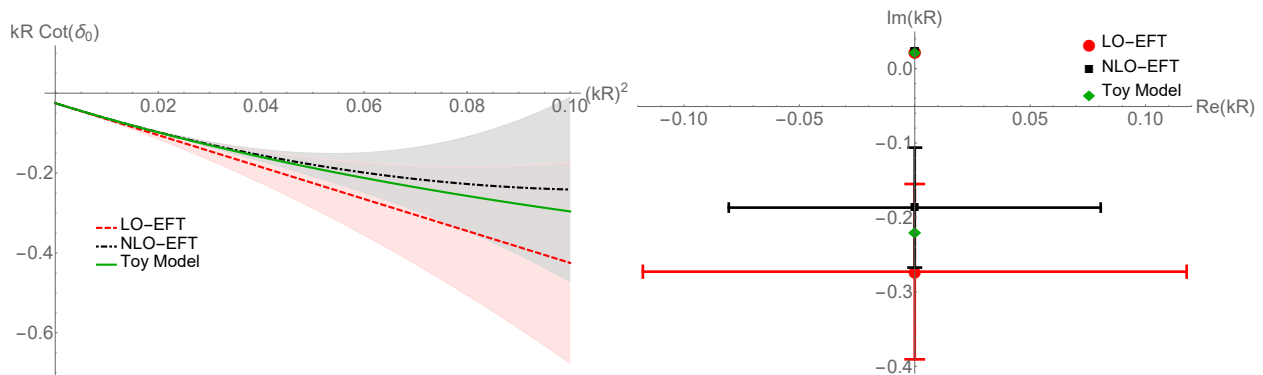


FIG. 6: Comparison between EFT and toy model for $kR \cot \delta_0$ as a function of $(kR)^2$ (left panel), and virtual- and bound-state pole positions on the complex kR plane (right panel), when $\alpha = 8.13476$ and $\beta^2 = 7.89592$. Notation as in Fig. 3.

	$k_1 R$	$k_2 R$
LO EFT	$(2.2902 \pm 0.0006) \times 10^{-2} i$	$-(0.3 \pm 0.1) i$
NLO EFT	$(2.289773 \pm 0.000003) \times 10^{-2} i$	$-(0.19 \pm 0.08) i$
Toy model	$2.2897717 \times 10^{-2} i$	$-0.218497385 i$

TABLE V: Position of bound and virtual poles $k_{1,2}$ in units of R^{-1} , when $\alpha = 8.13476$ and $\beta^2 = 7.89592$. The EFT at LO and NLO is compared with the toy model.

VI. CONCLUSION

We have constructed an effective field theory that describes the scattering of two nonrelativistic particles when two shallow S -wave poles are present. Resonant nonrelativistic scattering has been considered before in EFT [14–18], but only with energy-dependent interactions. The characteristic feature of our formulation is the sole reliance on momentum-dependent interactions, which are easier to employ in more-particle systems. The effective Lagrangian for any low-energy two-body scattering process involving short-range forces can be written as an expansion in contact operators with an increasing number of spatial derivatives. The challenge, which we met above, is to order these interactions with a power counting appropriate to produce resonant poles in the scattering amplitude.

It is well known that various observables — like the scattering length and the effective range in the effective-range expansion — reflect the presence of resonant states. This feature, which we have illustrated with a toy model against which we compare our EFT, motivates the power-counting scheme we use in this paper. We find that the low-energy scattering amplitude yields resonant poles only when the two leading operators in the derivative expansion are treated nonperturbatively. At higher orders, operators with an increasing number of derivatives contribute perturbatively. Our EFT successfully produces a controlled expansion about the resonant states and predicts the positions of poles with an error that can be systematically reduced by adding higher-dimensional operators. The same is true more generally for other situations involving two shallow S -wave poles, such as two virtual states, or one virtual state and one bound state.

As a *bona fide* EFT, ours obeys approximate renormalization-group invariance. It is remarkable that renormalization at leading order forces the effective range to be negative [24, 25]. This is in agreement with Wigner’s bound [26] and allows no more than one pole in the upper half of the complex momentum plane. Thus, renormalization automatically incorporates the causality constraint that a resonance represents decaying, not growing, states [1, 36]. It also does not allow for a redundant pole on the positive imaginary axis [39–41] nor for a double bound-state pole, which is excluded by other arguments [1, 36, 38]. In short, the resulting S matrix obeys the conditions expected on general grounds [1]. In contrast, the renormalization of the EFT with “dimer” auxiliary fields [14–18] allows for the more general situation, believed to be unphysical, where two (or more) shallow poles appear in the upper half-plane.

The situation does not change at higher orders, since the corrections are perturbative. The need to remove the residual cutoff dependence gives clues about the orders corrections come at. We saw explicitly how the four-derivative operator enters at next-to-leading order, gives rise to a known form for the S matrix [36], and improves on the leading-order description systematically. There is no obvious obstacle to continuing this process beyond next-to-leading order.

Power counting and renormalization here are significantly different than those [9–12] for a single shallow S -wave pole. The need to treat the two-derivative contact interaction perturbatively in the latter case has been known for a

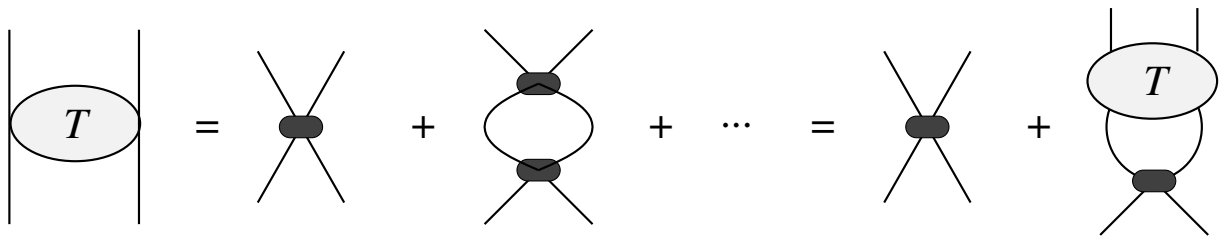


FIG. 7: The two-body T matrix as a sum of Feynman diagrams. Particle propagation (A1) is represented by a solid line, while the dark oval stands for the potential (3).

long time [9–12], but now we understand this need from the fact that the situation described by a nonperturbative treatment of the two-derivative contact interaction is different in a physically meaningful way — it corresponds to different regions of the parameter space of an underlying potential, or to a different type of potential altogether.

The EFT developed in this paper is directly applicable only to resonant S -wave scattering of two spin-zero particles that interact via a short-range force. Although at the two-body level it is equivalent to a particular ordering of the effective-range expansion, it is a Hamiltonian framework that allows for the investigation of the effects of this two-body physics in processes involving more than two particles. This is analogous to the single-pole theory, where for example the three-body system can be dealt with [49–53]. The next obvious step is to include spin and (in the nuclear case) isospin quantum numbers, as well as higher waves. Furthermore, we aim to study resonant scattering of electrically charged particles by including the long-range Coulomb interactions in our EFT. We anticipate that a nonperturbative treatment of the Coulomb interaction will be necessary to describe resonant scattering of alpha particles at low energies [16]. The EFT developed in this paper is a step in this direction.

Acknowledgments

UvK is grateful to R. Higa for useful discussions. This research was supported in part by the U.S. Department of Energy, Office of Science, Office of Nuclear Physics, under award number DE-FG02-04ER41338.

Appendix A: T matrix from Feynman diagrams

Here we obtain the T matrix in field theory by summation of Feynman diagrams. The potential (3) is represented by four-legged vertices with an increasing number of powers of momenta. Since antiparticles are integrated out, the two-body amplitude is just a string of these vertices connected by two single-particle propagators,

$$S_F(q) = \frac{i}{q_0 - \vec{q}^2/2m + i\epsilon} + \dots, \quad (\text{A1})$$

where q^0 (\vec{q}) is the fourth (three-dimensional) component of the particle's 4-vector and “...” represent relativistic corrections. We will neglect the latter here, but their inclusion poses no additional conceptual problems [12]. The sum of diagrams is shown in Fig. 7.

We can write the S -wave T matrix in a compact way by defining in ($|p\rangle$) and out ($|p'\rangle$) vectors and a vertex matrix (\mathcal{C}) through

$$|p\rangle \equiv \begin{pmatrix} 1 \\ p^2 \\ p^4 \\ \vdots \end{pmatrix}, \quad |p'\rangle \equiv \begin{pmatrix} 1 \\ p'^2 \\ p'^4 \\ \vdots \end{pmatrix}, \quad \mathcal{C} \equiv \frac{4\pi}{m} \begin{pmatrix} C_0 & C_2/2 & C_4/4 & \dots \\ C_2/2 & C_4/2 & 3C_6/8 & \dots \\ C_4/4 & 3C_6/8 & 3C_8/8 & \dots \\ \vdots & \vdots & \vdots & \ddots \end{pmatrix}. \quad (\text{A2})$$

(See also Ref. [27].) The tree diagram in Fig. 7 is then simply

$$T_{0,0}(p', p) = V(p', p) = \langle p' | \mathcal{C} | p \rangle. \quad (\text{A3})$$

The loop diagrams involve a 4-momentum integration. Since the vertices depend only on the 3-momenta, we can evaluate the q^0 integrals in the center-of-mass frame,

$$\int \frac{d^4 q}{(2\pi)^4} \bar{q}^{2n} \frac{i}{q^0 - \bar{q}^2/2m + i\epsilon} \frac{i}{k^2/2m - q^0 - \bar{q}^2/2m + i\epsilon} = -i \frac{m}{4\pi} I_{2n}^+, \quad (\text{A4})$$

where I_{2n}^+ is defined in Eq. (12). If we define a matrix of integrals,

$$\mathcal{I} \equiv -m \int \frac{d^3 q}{(2\pi)^3} \frac{|q\rangle\langle q|}{k^2 - q^2 + i\epsilon} = -\frac{m}{4\pi} \begin{pmatrix} I_0^+ & I_2^+ & I_4^+ & \cdots \\ I_2^+ & I_4^+ & I_6^+ & \cdots \\ I_4^+ & I_6^+ & I_8^+ & \cdots \\ \vdots & \vdots & \vdots & \ddots \end{pmatrix}, \quad (\text{A5})$$

the one-loop diagram takes the form

$$T_{0;1}(p', p) = -m \int \frac{d^3 q}{(2\pi)^3} \frac{V(p', q) V(q, p)}{k^2 - q^2 + i\epsilon} = \langle p' | \mathcal{C} \mathcal{I} \mathcal{C} | p \rangle. \quad (\text{A6})$$

With a regulator on nucleon momenta, the multiple-loop diagrams separate and the sum of diagrams is

$$T_0(p', p) = \sum_{i=0}^{\infty} T_{0;i}(p', p) = \langle p' | (\mathcal{C} + \mathcal{C} \mathcal{I} \mathcal{C} + \mathcal{C} \mathcal{I} \mathcal{C} \mathcal{I} \mathcal{C} + \dots) | p \rangle = \langle p' | \mathcal{C} (1 - \mathcal{I} \mathcal{C})^{-1} | p \rangle \equiv \langle p' | \mathcal{T}_0 | p \rangle. \quad (\text{A7})$$

Since predictive power requires a finite number of parameters at each order, we need to truncate the amplitude (A7) at different orders in order to renormalize it. The LO T matrix results from taking $C_0 = C_0^{(0)}$, $C_2 = C_2^{(0)}$, and $C_{n \geq 4} = 0$ in the matrix \mathcal{C} . We arrive at

$$\frac{4\pi}{mT_0^{(0)}(p', p)} = \frac{(4C_0^{(0)} - C_2^{(0)2} I_4) I_0 + (2 + C_2^{(0)} I_2)^2}{4C_0^{(0)} - C_2^{(0)2} I_4 + C_2^{(0)} (2 + C_2^{(0)} I_2) (p'^2 + p^2) - C_2^{(0)2} I_0 p'^2 p^2}, \quad (\text{A8})$$

which gives Eq. (16) on-shell, that is, when $p^2 = p'^2 = k^2$. To obtain the NLO T matrix, we take instead $C_0 = C_0^{(0)} + C_0^{(1)}$, $C_2 = C_2^{(0)} + C_2^{(1)}$, $C_4 = C_4^{(1)}$, and $C_{n \geq 6} = 0$, expanding in the subleading pieces. Retaining only terms linear in $C_{0,2,4}^{(1)}$ results on-shell in Eq. (29). The procedure can be continued in a straightforward way at higher orders.

Note that the same results can be obtained from Feynman diagrams in a form that is somewhat closer to the procedure of the main text. We rewrite the sum of diagrams (A7) as a Lippmann-Schwinger equation,

$$\langle p' | \mathcal{T}_0 | p \rangle = \langle p' | \mathcal{C} | p \rangle + \langle p' | \mathcal{C} \mathcal{I} \mathcal{T}_0 | p \rangle. \quad (\text{A9})$$

This form is also shown in Fig. 7. The Lippmann-Schwinger equation can be solved at LO [24] with an *ansatz* motivated by the momentum structure of Eq. (A6),

$$\mathcal{T}_0^{(0)} = \begin{pmatrix} \tau_0^{(0)} & \tau_2^{(0)} & 0 & \cdots \\ \tau_2^{(0)} & \tau_4^{(0)} & 0 & \cdots \\ 0 & 0 & 0 & \cdots \\ \vdots & \vdots & \vdots & \ddots \end{pmatrix}. \quad (\text{A10})$$

Inserting this form on both sides of Eq. (A9) and matching powers of momenta, one finds three algebraic equations for $\tau_{0,2,4}^{(0)}$. Solving these equations we again obtain Eq. (A8). At NLO, we expand both \mathcal{C} and \mathcal{T}_0 in Eq. (A9) to linear order. The NLO correction $\mathcal{T}_0^{(1)}$ appears both directly on the left-hand side and inside an integral on the right-hand side. To solve the resulting equation we make an *ansatz* analogous to (A10) but now including the sixth power of momenta.

Appendix B: Renormalization procedure

In this appendix we give some of the details of our renormalization procedure, at both LO and NLO. In either case we expand the amplitude calculated within the EFT in a power series in $k/\Lambda \ll 1$ as

$$\frac{4\pi}{mT_0(k)} = ik + \sum_{n=0}^{\infty} g_{2n} k^{2n}, \quad (\text{B1})$$

where the coefficients

$$g_{2n} = g_{2n}^{(0)} + g_{2n}^{(1)} + \dots \quad (\text{B2})$$

depend on the bare LECs $C_{2n}(\Lambda)$ and the cutoff Λ . Since g_{2n} encodes short-range physics, only integer powers of the energy appear in the expansion (B1). The only non-analytic behavior is represented by the unitarity term ik , which stems from the Schrödinger propagation. The $C_{2n}(\Lambda)$ are fixed by matching Eq. (B1) with the ERE in Eq. (1).

At LO, the amplitude is given by Eq. (16). The first four non-zero $g_{2n}^{(0)}$ are:

$$g_0^{(0)} = L_1 - \frac{1}{C_2^{(0)2} L_5 - 4C_0^{(0)}} \left(C_2^{(0)} L_3 + 2 \right)^2, \quad (\text{B3})$$

$$g_2^{(0)} = L_{-1} - C_2^{(0)} \frac{C_2^{(0)} L_3 + 4}{(C_2^{(0)2} L_5 - 4C_0^{(0)})^2} \left(C_2^{(0)} L_3 + 2 \right)^2, \quad (\text{B4})$$

$$g_4^{(0)} = L_{-3} - C_2^{(0)2} \frac{(C_2^{(0)} L_3 + 4)^2}{(C_2^{(0)2} L_5 - 4C_0^{(0)})^3} \left(C_2^{(0)} L_3 + 2 \right)^2, \quad (\text{B5})$$

$$g_6^{(0)} = L_{-5} - C_2^{(0)3} \frac{(C_2^{(0)} L_3 + 4)^3}{(C_2^{(0)2} L_5 - 4C_0^{(0)})^4} \left(C_2^{(0)} L_3 + 2 \right)^2. \quad (\text{B6})$$

The expressions for $g_{0,2}^{(0)}$ agree with those in Refs. [24, 25]. We demand that $g_{0,2}^{(0)}$ reproduce given values of the scattering length a_0 and effective range r_0 ,

$$g_0^{(0)} = \frac{1}{a_0}, \quad (\text{B7})$$

$$g_2^{(0)} = -\frac{r_0}{2}. \quad (\text{B8})$$

This is a set of two equations from which the two running values of $C_0^{(0)}$ and $C_2^{(0)}$ can be obtained in terms of the L_n and the observables a_0 and r_0 as

$$C_0^{(0)} = -\frac{L_5}{L_3^2} \left[1 \mp \frac{\sqrt{2}(a_0 L_1 - 1)}{\sqrt{-a_0^2(r_0 + 2L_{-1})L_3 + 2(a_0 L_1 - 1)^2}} \right]^2 + \frac{2a_0(a_0 L_1 - 1)}{a_0^2(r_0 + 2L_{-1})L_3 - 2(a_0 L_1 - 1)^2}, \quad (\text{B9})$$

$$C_2^{(0)} = -\frac{2}{L_3} \left[1 \mp \frac{\sqrt{2}(a_0 L_1 - 1)}{\sqrt{-a_0^2(r_0 + 2L_{-1})L_3 + 2(a_0 L_1 - 1)^2}} \right]. \quad (\text{B10})$$

Equations (19) and (20) follow upon expanding the expressions above for $a_0\Lambda \gg 1$ and $r_0\Lambda \gg 1$. In addition, $g_4^{(0)}$ gives the residual dependence shown in Eq. (23).

At NLO, the amplitude is given by Eq. (29). Once we expand in k/Λ the shifts in the first four g_{2n} are given by

$$g_0^{(1)} = -\frac{4}{(C_2^{(0)2}L_5 - 4C_0^{(0)})^2} \left\{ C_0^{(1)} (C_2^{(0)}L_3 + 2)^2 - C_2^{(1)} (C_2^{(0)}L_3 + 2) (C_2^{(0)}L_5 + 2C_0^{(0)}L_3) \right. \\ \left. + \frac{C_4^{(1)}}{4} \left[C_2^{(0)2} (C_2^{(0)}L_3 + 4) (L_5^2 - L_3L_7) - 4C_2^{(0)}L_7 + 4C_0^{(0)}L_5 (C_2^{(0)}L_3 - 2) + 8C_0^{(0)2}L_3^2 \right] \right\}, \quad (\text{B11})$$

$$g_2^{(1)} = \frac{8(C_2^{(0)}L_3 + 2)}{(C_2^{(0)2}L_5 - 4C_0^{(0)})^3} \left\{ C_0^{(1)}C_2^{(0)} (C_2^{(0)}L_3 + 2) (C_2^{(0)}L_3 + 4) \right. \\ \left. + C_2^{(1)} \left[C_2^{(0)} (C_2^{(0)}L_3 + 4) (C_2^{(0)}L_5 + 2C_0^{(0)}L_3) - C_2^{(0)2}L_5 + 4C_0^{(0)} \right] \right. \\ \left. + \frac{C_4^{(1)}}{4} \left[C_2^{(0)3} (C_2^{(0)}L_3 + 4) (L_5^2 - L_3L_7) + 2C_2^{(0)2}L_7 (C_2^{(0)}L_3 + 4) - 2C_0^{(0)}C_2^{(0)2}L_3L_5 \right. \right. \\ \left. \left. - 8C_0^{(0)2}L_3 (C_2^{(0)}L_3 + 3) \right] \right\}, \quad (\text{B12})$$

$$g_4^{(1)} = -\frac{4(C_2^{(0)}L_3 + 2)(C_2^{(0)}L_3 + 4)}{(C_2^{(0)2}L_5 - 4C_0^{(0)})^4} \left\{ 3C_0^{(1)}C_2^{(0)2} (C_2^{(0)}L_3 + 2) (C_2^{(0)}L_3 + 4) \right. \\ \left. - C_2^{(1)}C_2^{(0)} \left[3C_2^{(0)} (C_2^{(0)}L_3 + 4) (C_2^{(0)}L_5 + 2C_0^{(0)}L_3) - 4 (C_2^{(0)2}L_5 - 4C_0^{(0)}) \right] \right. \\ \left. + \frac{C_4^{(1)}}{4} \left[3C_2^{(0)4} (C_2^{(0)}L_3 + 6) (L_5^2 - L_3L_7) - 8C_2^{(0)3}L_7 + 4C_2^{(0)3}L_5 (C_0^{(0)}L_3 - 2C_2^{(0)}L_5) \right. \right. \\ \left. \left. + 32C_0^{(0)2} (C_2^{(0)}L_3 + 1) + 24C_0^{(0)2}C_2^{(0)}L_3 (C_2^{(0)}L_3 + 2) \right] \right\}, \quad (\text{B13})$$

$$g_6^{(1)} = -\frac{8(C_2^{(0)}L_3 + 2)(C_2^{(0)}L_3 + 4)^2}{(C_2^{(0)2}L_5 - 4C_0^{(0)})^5} C_2^{(0)} \left\{ 4C_0^{(1)}C_2^{(0)2} (C_2^{(0)}L_3 + 2) (C_2^{(0)}L_3 + 4) \right. \\ \left. - C_2^{(1)}C_2^{(0)} \left[2C_2^{(0)} (C_2^{(0)}L_3 + 4) (C_2^{(0)}L_5 + 2C_2^{(0)}L_3) - 3 (C_2^{(0)2}L_5 - 4C_0^{(0)}) \right] \right. \\ \left. + \frac{C_4^{(1)}}{2} \left[C_2^{(0)4} (C_2^{(0)}L_3 + 6) (L_5^2 - L_3L_7) + 8C_2^{(0)3}L_7 - C_2^{(0)3}L_5 (C_0^{(0)}L_3 - 3C_2^{(0)}L_5) \right. \right. \\ \left. \left. + 16C_0^{(0)2} (C_2^{(0)}L_3 + 1) + 4C_0^{(0)2}C_2^{(0)}L_3 (2C_2^{(0)}L_3 + 3) \right] \right\}. \quad (\text{B14})$$

Now we demand that the shape parameter P_0 be reproduced, without changes in the scattering length and effective ranges; that is, we impose

$$g_0^{(1)} = 0, \quad (\text{B15})$$

$$g_2^{(1)} = 0, \quad (\text{B16})$$

$$g_4^{(1)} = P_0 \left(\frac{r_0}{2} \right)^3 - g_4^{(0)}. \quad (\text{B17})$$

Solving for the three unknowns $C_{0,2,4}^{(1)}$ which appear linearly,

$$C_0^{(1)} = - \left(\frac{P_0 r_0^3}{8} - g_4^{(0)} \right) \frac{(C_2^{(0)2} L_5 - 4C_0^{(0)})^2}{16(C_2^{(0)} L_3 + 2)^2 (C_2^{(0)} L_3 + 4)} \left[C_2^{(0)2} (C_2^{(0)} L_3 + 4) (L_5^2 + L_3 L_7) + 4C_2^{(0)} L_7 \right. \\ \left. + 6C_0^{(0)} C_2^{(0)} L_3 L_5 (C_2^{(0)} L_3 + 4) + 4C_0^{(0)2} L_3^2 (C_2^{(0)} L_3 + 4) + 8C_0^{(0)} L_5 \right], \quad (\text{B18})$$

$$C_2^{(1)} = - \left(\frac{P_0 r_0^3}{8} - g_4^{(0)} \right) \frac{(C_2^{(0)2} L_5 - 4C_0^{(0)})^2}{8(C_2^{(0)} L_3 + 2)(C_2^{(0)} L_3 + 4)} \left[C_2^{(0)} L_5 (C_2^{(0)} L_3 + 4) + C_0^{(0)} L_3 (C_2^{(0)} L_3 + 6) \right], \quad (\text{B19})$$

$$C_4^{(1)} = - \left(\frac{P_0 r_0^3}{8} - g_4^{(0)} \right) \frac{(C_2^{(0)2} L_5 - 4C_0^{(0)})^2}{8(C_2^{(0)} L_3 + 4)}, \quad (\text{B20})$$

where $g_0^{(0)}$, $C_0^{(0)}$ and $C_2^{(0)}$ are given in Eqs. (B5), (B9) and (B10). Expanding these expressions for $a_0 \Lambda \gg 1$ and $r_0 \Lambda \gg 1$ we obtain Eqs. (33), (34), and (35). The residual cutoff dependence in Eq. (36) results from $g_6^{(0)} + g_6^{(1)}$.

-
- [1] C. Møller, Kgl. Danske Vid. Selsk. Mat.-Fys. Medd. **22** (1946) 19.
 - [2] J.R Taylor, *Scattering Theory: The Quantum Theory of Nonrelativistic Collisions*, Wiley, New York (1972).
 - [3] L.P. Kok, Phys. Rev. Lett. **45** (1980) 427.
 - [4] S.A. Afzal, A.A.Z. Ahmad, and S. Ali, Rev. Mod. Phys. **41** (1969) 247.
 - [5] S. Weinberg, Physica A **96** (1979) 327.
 - [6] S. Weinberg, Rev. Mod. Phys. **52** (1980) 515 [Science **210** (1980) 1212].
 - [7] P.F. Bedaque and U. van Kolck, Ann. Rev. Nucl. Part. Sci. **52** (2002) 339.
 - [8] H.-W. Hammer, S. König, and U. van Kolck, Rev. Mod. Phys. **92** (2020) 025004.
 - [9] U. van Kolck, Lect. Notes Phys. **513** (1998) 62.
 - [10] D.B. Kaplan, M.J. Savage, and M.B. Wise, Phys. Lett. B **424** (1998) 390.
 - [11] D.B. Kaplan, M.J. Savage, and M.B. Wise, Nucl. Phys. B **534** (1998) 329.
 - [12] U. van Kolck, Nucl. Phys. A **645** (1999) 273.
 - [13] D.B. Kaplan, Nucl. Phys. B **494** (1997) 471.
 - [14] C.A. Bertulani, H.-W. Hammer, and U. van Kolck, Nucl. Phys. A **712** (2002) 37.
 - [15] P.F. Bedaque, H.-W. Hammer, and U. van Kolck, Phys. Lett. B **569** (2003) 159.
 - [16] R. Higa, H.-W. Hammer, and U. van Kolck, Nucl. Phys. A **809** (2008) 171.
 - [17] B.A. Gelman, Phys. Rev. C **80** (2009) 034005.
 - [18] M.H. Alhakami, Phys. Rev. D **96** (2017) 056019.
 - [19] J. Rotureau and U. van Kolck, Few-Body Syst. **54** (2013) 725.
 - [20] C. Ji, C. Elster, and D.R. Phillips, Phys. Rev. C **90** (2014) 044004.
 - [21] E. Ryberg, C. Forssén, and L. Platter, Few-Body Syst. **58** (2017) 143.
 - [22] H.A. Bethe, Phys. Rev. **76** (1949) 38.
 - [23] U. van Kolck, Eur. Phys. J. A **56** (2020) 97.
 - [24] D.R. Phillips, S.R. Beane, and T.D. Cohen, Annals Phys. **263** (1998) 255.
 - [25] S.R. Beane, T.D. Cohen, and D.R. Phillips, Nucl. Phys. A **632** (1998) 445.
 - [26] E.P. Wigner, Phys. Rev. **98** (1955) 145.
 - [27] S. Beck, B. Bazak, and N. Barnea, Phys. Lett. B **806** (2020) 135485.
 - [28] T.D. Cohen, B.A. Gelman and U. van Kolck, Phys. Lett. B **588** (2004) 57.
 - [29] H. Georgi, Phys. Lett. B **240** (1990) 447.
 - [30] M.E. Luke and A.V. Manohar, Phys. Lett. B **286** (1992) 348.
 - [31] S. Fleming, T. Mehen, and I.W. Stewart, Nucl. Phys. A **677** (2000) 313.
 - [32] I. Stetcu, J. Rotureau, B.R. Barrett, and U. van Kolck, Annals Phys. **325** (2010) 1644.
 - [33] C.J. Fewster, J. Phys. A **28** (1995) 1107.
 - [34] D.R. Phillips and T.D. Cohen, Phys. Lett. B **390** (1997) 7.
 - [35] R.E. Peierls, Proc. Roy. Soc. (London) A **253** (1959) 16.
 - [36] N. Hu, Phys. Rev. **74** (1948) 131.
 - [37] W. Schützer and J. Tiomno, Phys. Rev. **83** (1951) 249.
 - [38] Y.N. Demkov and G.F. Drukarev, Sov. Phys. JETP **22** (1966) 479.
 - [39] S.T. Ma, Phys. Rev. **69** (1946) 668.
 - [40] D. ter Haar, Physica **12** (1946) 501.
 - [41] S.T. Ma, Phys. Rev. **71** (1947) 195.

- [42] C. Nelson, A. Rajagopal, and C. Shastri, *J. Math. Phys.* **12** (1971) 737.
- [43] P. Terry, *J. Math. Phys.* **23** (1982) 87.
- [44] V. Bargmann, *Phys. Rev.* **75** (1949) 301.
- [45] K. Yamamoto, *Prog. Theor. Phys.* **27** (1962) 219.
- [46] T. Mehen and I.W. Stewart, *Phys. Lett. B* **445** (1999) 378.
- [47] N.G. van Kampen, *Phys. Rev.* **91** (1953) 1267.
- [48] H.M. Nussenzweig, *Nucl. Phys.* **11** (1959) 499.
- [49] P.F. Bedaque and U. van Kolck, *Phys. Lett. B* **428** (1998) 221.
- [50] P.F. Bedaque, H.-W. Hammer, and U. van Kolck, *Phys. Rev. C* **58** (1998) 641.
- [51] P.F. Bedaque, H.-W. Hammer, and U. van Kolck, *Phys. Rev. Lett.* **82** (1999) 463.
- [52] P.F. Bedaque, H.-W. Hammer, and U. van Kolck, *Nucl. Phys. A* **646** (1999) 444.
- [53] P.F. Bedaque, H.-W. Hammer, and U. van Kolck, *Nucl. Phys. A* **676** (2000) 357.